

## Long-wavelength instabilities of three-dimensional patterns

T. K. Callahan<sup>1,2\*</sup> and E. Knobloch<sup>1†</sup>

<sup>1</sup>*Department of Physics, University of California, Berkeley, California 94720*

<sup>2</sup>*Department of Mathematics, University of Michigan, Ann Arbor, Michigan 48109*

(Received 24 May 1999; revised manuscript received 24 April 2000; published 28 August 2001)

Long-wavelength instabilities of steady patterns, spatially periodic in three dimensions, are studied. All potentially stable patterns with the symmetries of the simple-, face-centered- and body-centered-cubic lattices are considered. The results generalize the well-known Eckhaus, zigzag, and skew-varicose instabilities to three-dimensional patterns and are applied to two-species reaction-diffusion equations modeling the Turing instability.

DOI: 10.1103/PhysRevE.64.036214

PACS number(s): 89.75.Kd, 47.20.Ky, 47.54.+r

### I. INTRODUCTION

Formation of structure via spontaneous symmetry-breaking bifurcations is a topic of much current interest [1]. Despite this, little work has been done on pattern formation in three dimensions, i.e., in systems that are translation invariant in three dimensions. The recent experimental discovery of the Turing instability [2,3] provides one motivation for extending the existing theory for two-dimensional patterns to three dimensions. The Turing instability arises in reaction-diffusion systems and the characteristic wavelength of the pattern that is produced is *intrinsic*, i.e., it depends only upon the reaction rates, concentrations, and diffusivities of the chemicals involved, and not upon any externally imposed length scale. Thus if the dimensions of the experimental apparatus are much larger than the intrinsic length scale, the instability can develop free from the influence of boundaries and produce truly three-dimensional patterns. Other systems exhibiting pattern formation in three dimensions include block copolymer melts [4] and parametric oscillators in optics [5]. In the former a polymer consisting of long blocks of different monomers starts in a spatially uniform state. As time progresses, the different monomer types self-segregate into distinct domains, frequently with spatial periodicity. Both systems produce spatial structures that are similar to those predicted by the general theory for three-dimensional patterns on spatially periodic cubic lattices [6,7]. This analysis focuses on the vicinity of a steady state instability in generic systems with translation invariance in three dimensions, and determines the types of spatially periodic patterns with the symmetry of the different types of cubic lattices and their stability properties with respect to perturbations on these lattices, but other types of perturbations have not been considered. In particular the stability properties of the predicted stable states with respect to long-wavelength perturbations remain unknown. In two dimensions such perturbations are known to be important in so far as they are involved in the various instabilities (such as the Eckhaus, zigzag, and skew-varicose instabilities) that restrict the possible wavelength of the pattern. These instabilities, originally identified

in the stability theory for convective rolls, are generic in the sense that they destabilize roll-like states in all continuum systems with Euclidean symmetry in two dimensions.

Calculations of this type provide useful information even about systems that do not strictly satisfy all the hypotheses used to construct the theory. The Turing instability is a case in point. Actual experiments on Turing structures involve concentration gradients of the feed chemicals, which necessarily break both the homogeneity and the isotropy of the system. This is the case, for example, in the experiments reported in Refs. [2] and [3] in which the feed gradient was imposed *in the plane* of the observed patterns and not perpendicular to it as in subsequent experiments. Despite this the hexagons that were predicted for a homogeneous system were still found. Thus a study of the corresponding problem in three dimensions should likewise produce useful results. In fact, because the characteristic length scale of the instability is so much smaller than all the external dimensions, the authors of Refs. [2] and [3] conclude that the observed structures must in fact be three-dimensional and that the top-view hexagonal pattern is actually a two-dimensional projection of a body-centered-cubic (bcc) structure. More recently, two-dimensional black-eye patterns in reaction-diffusion systems have also been explained in terms of sections of a three-dimensional bcc structure [8]. The block copolymer melts investigated in Ref. [4] do not suffer from these limitations of the theory.

It is important, therefore, that the methods used to study pattern formation and stability in two dimensions be extended to the three-dimensional case. For patterns on a spatially periodic three-dimensional lattice the equivariant bifurcation theory approach has led to an almost complete description of the possible stationary patterns on the simple-cubic (sc), face-centered-cubic (fcc), and bcc lattices and their stability properties with respect to all perturbations on these lattices [6,7]. Near onset these patterns are described by (real) functions of the form

$$\psi(\vec{x}) = \sum_{i=1}^N z_i e^{i\vec{k}_i \cdot \vec{x}} + \text{c.c.} + \text{n.l.t.}, \quad (1.1)$$

where  $|\vec{k}_i| = k_c$ ,  $i = 1, \dots, N$  and  $N = 3, 4$ , and  $6$ , respectively. The shorthand n.l.t. represents terms that are nonlinear

\*Email address: timcall@math.lsa.umich.edu

†Email address: knobloch@physics.berkeley.edu

in the complex amplitudes  $z_i$ ; these satisfy appropriate amplitude equations and thereby specify the possible patterns.

In this paper we extend these calculations to examine the stability properties of patterns with wave numbers that differ from the optimum wave number selected at onset, focusing on *phase* instabilities. As in one- and two-dimensional patterns these instabilities limit the wavelength of stable spatially periodic patterns, leading (in two dimensions) to the so-called Busse balloon. The instabilities arise either as a result of the destabilization of neutrally stable translation modes by long-wavelength perturbations or due to long-wavelength symmetry-breaking bifurcations. Because of their long-wavelength nature both types of instabilities are easily identified. In one dimension the stability limit is provided by the well-known Eckhaus instability. This instability is identified as follows. Near onset the evolution of an amplitude  $z(t)$  of a mode with wave number  $k$  in a left-right symmetric system is described by the amplitude equation

$$\dot{z} = [\lambda - \delta(k - k_c)^2]z + a|z|^2z + \dots, \quad (1.2)$$

where  $\lambda$  is the bifurcation parameter ( $|\lambda| \ll 1$ ) and  $\delta > 0$  and  $a < 0$  are real, model-dependent coefficients. This mode has a linear growth rate  $\lambda - \delta(k - k_c)^2$ , and thus the trivial state is unstable to any mode  $k$  with

$$\delta(k - k_c)^2 < \lambda.$$

Only some of these wave numbers, however, can appear as stable patterns. To see which wave numbers, consider a mode of wave number  $k = k_c + q$ , with  $q$  small, corresponding to a *space-dependent* amplitude of the critical mode

$$z(x, t) = r e^{iqx}.$$

Equation (1.2) implies that at equilibrium  $r^2 = -(\lambda - \delta q^2)/a$ . Note that  $|\lambda| \ll 1$  implies that  $|q| \ll 1$ . This *distorted* state is linearly unstable with respect to perturbations with wave number  $k'$ ,  $|k'| \ll |q|$  if  $\delta q^2 < \lambda < 3\delta q^2$  [1], i.e., when  $\lambda > 0$  the trivial state is unstable to modes with  $q^2 < \lambda/\delta$  but if  $\lambda/3\delta < q^2 < \lambda/\delta$  these modes are themselves unstable on an even longer time scale. Thus only states with  $q^2 < \lambda/3\delta$  are stable. For larger  $q$  the instability shifts the locations of the maxima and minima of the pattern, thereby altering its wave number. The long term result is a slow distortion of the pattern until it becomes stable with respect to long-wavelength perturbations, i.e., until the system adjusts its wave number to one within the acceptable range  $q^2 < \lambda/3\delta$ . This usually occurs via phase slips that occur at locations where the amplitude  $z(x, t)$  passes through zero [9]. Only at the band center ( $q = 0$ ) is the one-dimensional pattern stable for all supercritical  $\lambda$ .

The above description applies equally to Rayleigh-Bénard rolls and Taylor-Couette vortices, which are two-dimensional fluid states but in which the transverse (i.e., bounded) dimension is “trivial.” These states are therefore effectively one-dimensional and the Eckhaus instability they undergo is a consequence of the destabilization of a neutral mode corresponding to translation of the pattern in the direction of its wave vector. For patterns, such as rolls in a plane, that are

invariant under translations in one direction, a different instability can take place. This is the zigzag instability and it breaks the translation invariance of the pattern along the roll axis. The skew-varicose instability can be thought of as a combination of these two fundamental instabilities; for this instability the associated displacement vector is neither parallel nor perpendicular to  $\vec{k}'$ . In contrast, a square pattern in a plane is two-dimensional in a nontrivial way, because it breaks translation invariance in *two* independent directions. Such patterns have two neutral directions (hereafter phase directions) and consequently their stability properties are described by a *pair* of coupled phase equations. As a result a square pattern also undergoes two types of instability, but this time both are associated with the destabilization of a neutral mode. Despite this difference in their origin we follow customary terminology and refer to these as the Eckhaus instability (present for  $\lambda < \text{const} \times q^2$ ) and the zigzag instability (present for  $q < 0$ ) [10]. For hexagons, analysis of the type described in Refs. [11] and [12] shows that the region of stability in the  $q$ - $\lambda$  plane—the *Busse balloon*—is completely closed by long-wavelength instabilities alone. This result is particularly significant in those cases in which the hexagons do *not* lose stability to rolls with increasing  $\lambda$ , since nothing beyond long-wavelength theory is required to bound the Busse balloon. We show here that this property is shared by the hexagonal prism and bcc states present in models of the Turing instability. For these and other three-dimensional patterns, the possibilities for instability are yet richer and these are described here in detail. It should also be mentioned that additional instabilities, the so-called amplitude instabilities, may be present. These include the cross-roll and oblique cross-roll instabilities of rolls. These instabilities select a stable wave number by destroying the existing pattern and regrowing a new one with a different orientation and a more favorable wavelength. Such amplitude instabilities may under appropriate circumstances provide a more stringent limit on the range of stable wave numbers than the phase instabilities alone [11].

The traditional methods for studying this problem in two dimensions, such as the Newell-Whitehead-Segel approach [13], lead to envelope equations that break the isotropy of the whole system. This is a consequence of rigorous adherence to asymptotics, which can only describe roll structures that are near a straight roll pattern with the same orientation *everywhere*. However, recently Gunaratne [14] introduced a new procedure characterized by a strict adherence to symmetry (in this case isotropy) at the expense of retaining certain formally small terms. Gunaratne demonstrated by numerical simulations that his procedure allows substantial changes in orientation of the patterns over large distances and that it provides a better qualitative description of the modulation of roll patterns than the traditional asymptotic procedure, at least when compared with experiments and direct numerical simulation of pattern-forming systems. Of course this is because the calculations are never in fact performed in the asymptotic regime. But the point remains that even in the asymptotic regime the traditional theory is unable to describe changes in roll orientation over arbitrarily large distances. In this paper we therefore adopt Gunaratne’s approach and gen-

eralize it to three-dimensional perturbations. In fact this approach is ideally suited to three dimensions and because it respects isotropy, it allows a relatively straightforward analysis of the resulting modulation equations.

In Sec. II we briefly describe Gunaratne's approach and introduce his "covariant" derivative  $\square_i$ . In Secs. III, IV, and V we solve the resulting modulation equations for the three cubic lattices of interest and determine which solutions may be expected to be stable in each of these cases. In the bcc case stable small amplitude solutions are present only when the quadratic terms in the amplitude equations are small. This is the case, in appropriate parameter regimes, for the two models of the Turing instability described in Sec. VI. Although this paper is motivated by the Turing instability we adopt a model-independent approach throughout, and we emphasize that the results are therefore applicable to *any* three-dimensional pattern-forming system with the appropriate periodicity. In Sec. VII we point out certain similarities among the calculations for the different solutions and summarize these in terms of general statements about pattern formation in higher-dimensional systems. Since our analysis involves the computation of eigenvalues of Hermitian matrices we find it convenient to employ quantum mechanical perturbation theory and the associated Dirac bra-ket notation [15].

## II. ENVELOPE EQUATIONS IN THREE DIMENSIONS

In this section we consider a general system of isotropic partial differential equations undergoing a steady state instability in three dimensions. Isotropy implies that the neutral stability curve takes the form

$$\lambda = f(k^2).$$

It follows that instability sets in at  $\lambda_c \equiv f(k_c^2)$ , where  $f'(k_c^2) = 0$  provided  $f''(k_c^2) > 0$ . In the following we assume that  $k_c > 0$  so that the instability has a finite wavelength. We are interested in patterns that form for slightly supercritical values of  $\lambda$  and with wave vectors  $\tilde{k}$ , whose lengths are close to  $k_c$ . In the following we choose a length scale such that  $k_c = 1$  and write  $\tilde{k} \equiv \hat{k} + \vec{q}$ , where  $|\hat{k}| = 1$ . Thus

$$\lambda - \lambda_c = \sum_{n=2}^{\infty} \frac{1}{n!} f^{(n)}(k_c^2) [2\hat{k} \cdot \vec{q} + q^2]^n.$$

The terms on the right side of this equation are responsible for the presence of the (slow) spatial derivatives in the (linearized) amplitude equation. These are obtained by replacing  $\vec{q}$  with  $-i\vec{\nabla}$ , resulting in the contribution

$$\sum_{n=2}^{\infty} \frac{1}{n!} f^{(n)}(k_c^2) (-2i)^n \square^n z_i,$$

where

$$\square \equiv \hat{k} \cdot \vec{\nabla} - \frac{i}{2} \nabla^2,$$

and  $z_i$  is now a function of a (slow) spatial variable  $\vec{x}$ . As emphasized by Gunaratne [14] the operator  $\square$  is rotationally invariant. To see what we mean by this, consider the amplitude equation for a roll pattern with wave number in the  $\hat{k}_1$  direction, say. Such a pattern is described by  $\text{Re}[A_1 e^{i\hat{k}_1 \cdot \vec{x}}]$ . This orientation is arbitrary, of course, and we would like to require that a rotation of this state through an angle  $\theta$ , which takes the amplitude  $A_1$  into  $A_1 e^{i\Delta\hat{k}_1 \cdot \vec{x}}$ , should be another solution to the envelope equation. Here  $\Delta\hat{k}_1 = \mathbf{R}_\theta \hat{k}_1 - \hat{k}_1$ , where  $\mathbf{R}_\theta$  is the rotation matrix. This is equivalent to the requirement

$$\square_1 e^{i\Delta\hat{k}_1 \cdot \vec{x}} = 0.$$

This condition is satisfied by  $\square_1 = \hat{k}_1 \cdot \vec{\nabla} - (i/2)\nabla^2$ , but not by its truncation to  $\hat{k}_1 \cdot \vec{\nabla}$ . Consequently, if we wish to retain the isotropy of the Euclidean group we must expand all quantities in powers of  $\square$  and not in powers of  $\vec{q}$  as obtained from the traditional asymptotic approach: in the latter approach any truncation breaks isotropy and hence a fundamental symmetry of the pattern-forming system. In the following we will therefore truncate our expansion to lowest order in  $\square$ , and not in  $\vec{q}$ . For example, retaining all terms of the form  $\square^m z^n$  with  $m+n \leq 3$ , Eq. (1.2) becomes

$$\dot{z} = \lambda z + a|z|^2 z + \delta \square^2 z + O(\square^4, z^4), \quad (2.1)$$

where  $O(\square^4, z^4)$  indicates terms of the form  $\square^m z^n$  with  $m+n \geq 4$ . A formal justification of the resulting equation [a modification of the Newell-Whitehead-Segel (NWS) equation] has been given by Graham [16]. However, sufficiently near onset, this modification has no qualitative effect and one still finds that the Eckhaus instability is present for wave numbers in the range  $\lambda/3\delta < q^2 < \lambda/\delta$ . In fact, as discussed further below, the use of envelope equations truncated uniformly at order  $O(\square^3, z^3)$  has only a benign effect on the stability boundaries of all spatially uniform patterns, even in two and three dimensions, although in two dimensions significant qualitative differences between the two truncations arise when these are used to study domain boundaries [14]. Rather than say that the inclusion of the higher order terms creates an extra symmetry that we would like, we prefer to say that the neglect of these terms violates a symmetry that the physical problem manifestly possesses.

On the bcc lattice the presence of a quadratic equivariant (see below) allows the addition of terms that are quadratic in the amplitudes  $z_i$  containing one factor of  $\square$ , cf. Ref. [17]. We do not consider this possibility here.

## III. THE SC LATTICE

The sc lattice is generated by the six wave vectors  $\pm \vec{k}_i$ ,  $i=1,2,3$ , taken from the sphere of marginally stable wave vectors, where

$$\hat{k}_1 = \hat{x}, \quad \hat{k}_2 = \hat{y}, \quad \hat{k}_3 = \hat{z}$$

TABLE I. Maximal isotropy branches for the sc lattice. Here  $\sigma_1 \equiv \sum_{i=1}^3 |z_i|^2$ .

Name	Solution	$\sigma_1$	Branching equation
Trivial	(0,0,0)	0	$\sigma_1=0$
Lamellas	(x,0,0)	$x^2$	$\lambda + (h_{1,\sigma_1} + h_3)\sigma_1=0$
Square prisms	(x,x,0)	$2x^2$	$\lambda + \frac{1}{2}(2h_{1,\sigma_1} + h_3)\sigma_1=0$
Simple cubic	(x,x,x)	$3x^2$	$\lambda + \frac{1}{3}(3h_{1,\sigma_1} + h_3)\sigma_1=0$

are unit vectors in Cartesian coordinates  $(x,y,z)$ . With the spatially dependent terms added, the (truncated) envelope equations take the form [7]

$$\dot{z}_1 = \lambda z_1 + (h_{1,\sigma_1} + h_3)|z_1|^2 z_1 + h_{1,\sigma_1}(|z_2|^2 + |z_3|^2)z_1 + \delta \square_1^2 z_1 + O(\square^4, \mathbf{z}^4), \quad (3.1)$$

where  $\mathbf{z} = (z_1, z_2, z_3)$ , together with two other equations obtained by cyclic permutation. Here  $\lambda \ll 1$  is a (real) bifurcation parameter, while  $h_{1,\sigma_1}$ ,  $h_3$ , and  $\delta > 0$  are real coefficients. Although the coefficient  $\delta$  can be scaled out by rescaling time and  $\lambda$  (the choice  $k_c = 1$  fixes the length scale) we retain it in what follows, in order to compare the results for  $q \neq 0$  with those listed in Table I for the *same*  $\lambda$  but at the band center ( $q = 0$ ). We are only interested in those solutions that can be stable with respect to perturbations on the sc lattice, i.e., simple-cubic patterns (hereafter sc) and lamellas (rolls) [7].

For supercritical values of  $\lambda$  all wave vectors within a spherical annulus become unstable and spatially periodic patterns with different values of  $|\vec{k}_j|$  may be constructed. As in Sec. I these correspond to distorted patterns of the form

$$z_i(\vec{x}, t) = e^{i\vec{q}_i \cdot \vec{x}} r_i,$$

where the  $\vec{q}_i$  denote small but arbitrary changes of the amplitude and direction of the lattice wave vectors (hereafter referred to as *distortions* of the lattice) and the  $r_j$  satisfy

$$\lambda + (h_{1,\sigma_1} + h_3)r_1^2 + h_{1,\sigma_1}(r_2^2 + r_3^2) - \delta[\hat{k}_1 \cdot \vec{q}_1 + \frac{1}{2}q_1^2]^2 = O(q^3, r^3) \quad (3.2)$$

and permutations. Note that the patterns on distorted lattices remain periodic, but with the lengths and angles of the wave vectors slightly altered. In the following we write

$$[\hat{k}_i \cdot \vec{q}_i + \frac{1}{2}q_i^2]^2 = \frac{1}{4}[(\hat{k}_i + \vec{q}_i)^2 - 1]^2 = \frac{1}{4}(\tilde{k}_i^2 - 1)^2, \quad (3.3)$$

where  $\tilde{k}_i \equiv \hat{k}_i + \vec{q}_i$ ,  $i = 1, 2, 3$ . To determine the stability of such distorted patterns with respect to long-wavelength perturbations we let

$$z_i(\vec{x}, t) = e^{i\vec{q}_i \cdot \vec{x}} [r_i + \alpha_i(t) e^{i\vec{k}' \cdot \vec{x}} + \bar{\beta}_i(t) e^{-i\vec{k}' \cdot \vec{x}}], \quad (3.4)$$

where  $\vec{k}'$  represents the perturbation wave vector  $|\vec{k}'| \ll |\vec{q}_i| \ll 1$ ,  $i = 1, 2, 3$ , and linearize the resulting equations in  $\alpha_i$ ,  $\beta_i$ .

### A. The solution sc

We first look at the sc solution, for which  $z_1 = z_2 = z_3 \equiv r$ . In order that this solution be stable with respect to perturbations on the sc lattice, we assume that (see below)

$$h_3 < 0, \quad 3h_{1,\sigma_1} + h_3 < 0, \quad \lambda - \delta q^2 > 0. \quad (3.5)$$

We consider uniformly distorted sc states, i.e., states with  $|\tilde{k}_1| = |\tilde{k}_2| = |\tilde{k}_3| \equiv \tilde{k}$ , say, but do not demand that the  $\vec{q}_i$  are necessarily parallel to the  $\hat{k}_i$ . Such states are given by

$$\lambda + (3h_{1,\sigma_1} + h_3)r^2 - \frac{1}{4}\delta(\tilde{k}^2 - 1)^2 = 0. \quad (3.6)$$

Perturbations of this distorted equilibrium evolve according to the linearized equations

$$\begin{aligned} \dot{\alpha}_1 &= (h_{1,\sigma_1} + h_3)r^2(\alpha_1 + \beta_1) + h_{1,\sigma_1}r^2(\alpha_2 + \beta_2) \\ &+ h_{1,\sigma_1}r^2(\alpha_3 + \beta_3) - \delta\alpha_1[(\tilde{k}_1^2 - 1)\tilde{k}_1 \cdot \vec{k}' + (\tilde{k}_1 \cdot \vec{k}')^2 \\ &+ \frac{1}{2}(\tilde{k}_1^2 - 1)k'^2] + O(k'^3; q^3, r^3), \end{aligned}$$

where  $O(k'^3; q^3, r^3)$  indicates terms of the form  $k'^l q^m r^n$  with  $l \geq 3$  or  $m + n \geq 3$ . The equation for  $\dot{\beta}_1$  is obtained by replacing  $\vec{k}'$  by  $-\vec{k}'$  and exchanging  $\alpha_i$  and  $\beta_i$ , while those for  $\dot{\alpha}_2, \dots, \dot{\beta}_3$  are obtained by permutation.

With the basis  $\xi = (\alpha_1, \beta_1, \alpha_2, \beta_2, \alpha_3, \beta_3)$ , the linearization of our system becomes

$$\dot{\xi} = (\mathbf{H}_0 + \mathbf{H}_1 + \mathbf{H}_2 + \mathbf{H}_3)\xi,$$

where

$$\mathbf{H}_0 = r^2 \begin{pmatrix} \mathbf{P} & \mathbf{Q} & \mathbf{Q} \\ \mathbf{Q} & \mathbf{P} & \mathbf{Q} \\ \mathbf{Q} & \mathbf{Q} & \mathbf{P} \end{pmatrix}, \quad \mathbf{P} = (h_{1,\sigma_1} + h_3) \begin{pmatrix} 1 & 1 \\ 1 & 1 \end{pmatrix}, \\ \mathbf{Q} = h_{1,\sigma_1} \begin{pmatrix} 1 & 1 \\ 1 & 1 \end{pmatrix},$$

$$\mathbf{H}_1 = -\delta(\tilde{k}^2 - 1) \begin{pmatrix} \mathbf{K}_1 & & \\ & \mathbf{K}_2 & \\ & & \mathbf{K}_3 \end{pmatrix},$$

$$\mathbf{K}_i = (\tilde{k}_i \cdot \vec{k}') \begin{pmatrix} 1 & \\ & -1 \end{pmatrix},$$

$$\mathbf{H}_2 = -\delta \begin{pmatrix} \mathbf{K}_1^2 & & \\ & \mathbf{K}_2^2 & \\ & & \mathbf{K}_3^2 \end{pmatrix},$$

$$\mathbf{H}_3 = -\frac{\delta}{2}(\tilde{k}^2 - 1)k'^2 \mathbf{1}.$$

Here  $\mathbf{H}_0$  is  $O(r^2) = O(q^2) = O(\lambda)$ ,  $\mathbf{H}_1$  is  $O(qk')$ ,  $\mathbf{H}_2$  is  $O(k'^2)$ , and  $\mathbf{H}_3$  is  $O(qk'^2)$ . In the following we work to  $O(k'^2)$  and drop terms of  $O(qk'^2)$ . Since the matrix  $\mathbf{H}_0 + \mathbf{H}_1 + \mathbf{H}_2 + \mathbf{H}_3$  is real symmetric all its eigenvalues are real and there are no Hopf bifurcations.

The (orthogonal) eigenvectors of  $\mathbf{H}_0$  are the columns of

$$\Phi = (\phi_1, \dots, \phi_6) = \begin{pmatrix} -1 & 0 & 0 & 1 & 1 & 1 \\ 1 & 0 & 0 & 1 & 1 & 1 \\ 0 & -1 & 0 & -1 & 1 & 1 \\ 0 & 1 & 0 & -1 & 1 & 1 \\ 0 & 0 & -1 & 0 & -2 & 1 \\ 0 & 0 & 1 & 0 & -2 & 1 \end{pmatrix}$$

with eigenvalues

$$\{e_i\}_{i=1, \dots, 6} = r^2 \{0, 0, 0, 2h_3, 2h_3, 2(3h_{1,\sigma_1} + h_3)\},$$

respectively. These are the stability eigenvalues of the sc state with respect to perturbations on the sc lattice. The inequalities (3.5) guarantee that the last three eigenvalues are negative, so that the eigenvectors  $|\phi_4\rangle$ ,  $|\phi_5\rangle$ , and  $|\phi_6\rangle$  are stable and remain so for small  $\tilde{k}'$ . In the following we employ quantum mechanical perturbation theory and the Dirac bra-ket notation, so that  $|\phi_4\rangle$  is a column vector and  $\langle\phi_4|$  is the row vector, i.e., the transpose conjugate of  $|\phi_4\rangle$ , etc. To determine whether the first three eigenvectors remain stable when  $k' \neq 0$ , we must look at terms of higher order in  $k'/q$ .

Before proceeding we examine the physical interpretation of the null eigenvectors of  $\mathbf{H}_0$ . Suppose we find that the state  $\alpha_i = \beta_i = 0$  loses stability to the eigenvector  $|\phi_1\rangle$ . What effect does this have on the sc state? The values of  $\alpha_1$  and  $\beta_1$  start to grow from 0 with  $\alpha_1 = -\beta_1 = |\alpha_1|e^{i\varphi}$ . While these are still extremely small we have, approximately,

$$z_1 = e^{i\tilde{q}_1 \cdot \tilde{x}} [r + \alpha_1 e^{i\tilde{k}' \cdot \tilde{x}} - \bar{\alpha}_1 e^{-i\tilde{k}' \cdot \tilde{x}}] \\ \approx r \exp \left\{ i \left[ \tilde{q}_1 \cdot \tilde{x} + \frac{2|\alpha_1|}{r} \sin(\tilde{k}' \cdot \tilde{x} + \varphi) \right] \right\}.$$

One way to interpret this result is to look at the positions of the maxima of the pattern. We know from Ref. [7] that the positions of the maxima of the sc solution form a simple-cubic lattice. At leading order the pattern is defined by the scalar function

$$\psi(\tilde{x}) = \sum_{i=1}^3 z_i e^{i\tilde{k}_i \cdot \tilde{x}} + \text{c.c.},$$

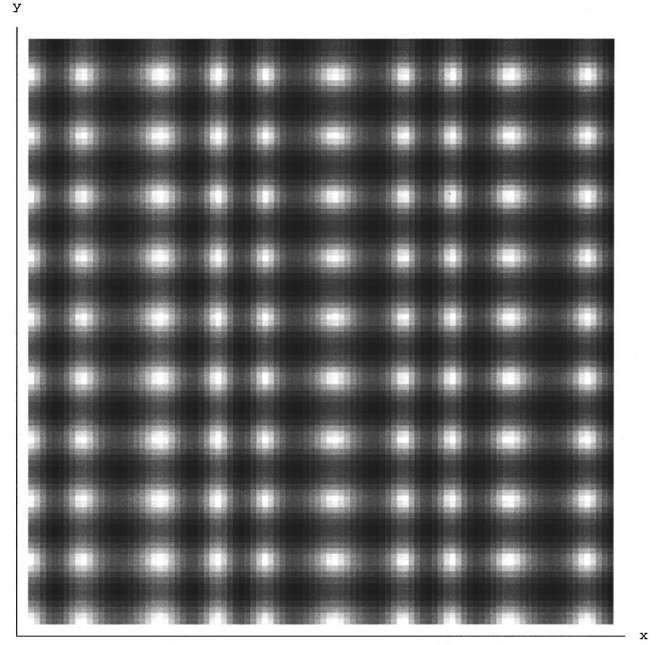


FIG. 1. The Eckhaus instability in the  $x$ - $y$  plane. The unperturbed solution has maxima (white) at the vertices of a square lattice and minima (black) at the vertices of another square lattice. Thus the unperturbed solution could be the sc or square prism solutions (or squares on the two-dimensional square lattice). For the Eckhaus instability, the displacements of the maxima are parallel to the modulation wave vector  $\tilde{k}'$ , here both in the  $x$  direction.

and the maxima are found by requiring that

$$(\hat{k}_i + \tilde{q}_i) \cdot \tilde{x} + \frac{2|\alpha_1|}{r} \sin(\tilde{k}' \cdot \tilde{x} + \varphi) = 2n_i\pi, \quad n_i \in \mathbb{Z},$$

with  $|\alpha_1| \ll r$ . The effect of the proposed long-wavelength perturbation is to shift the positions of the maxima slightly from their original ( $\alpha_1 = 0$ ) locations. Since only  $z_1$  is affected, the maxima are shifted in the  $\tilde{k}_1 \approx \hat{k}_1 = \hat{x}$  direction; this shift is periodic with wave vector  $\tilde{k}'$ . If  $\tilde{k}' \parallel \tilde{k}_1$  the shifts form a “longitudinal” wave, with alternating regions of compression and rarefaction of the maxima. This is the Eckhaus instability, and is illustrated in Fig. 1. The figure shows a cross section through the  $x$ - $y$  plane. If  $\tilde{k}' \perp \tilde{k}_1$ , the perturbation is “transverse,” with maxima shifted at right angles to the modulation wave vector. This is the zigzag instability, and is illustrated in Fig. 2. If neither of these relationships holds, the instability is called skew varicose, an example of which is shown in Fig. 3.

All of the modes for which  $\alpha_i = -\beta_i$  can be interpreted as modulations of the phase, and we will refer to these as PM modes. Modes for which  $\alpha_i = +\beta_i$  can analogously be interpreted as modulations of the amplitude of the pattern, and we refer to these as AM modes.

Since the operation  $\tilde{k}' \rightarrow -\tilde{k}'$  merely exchanges  $\alpha_i$  and  $\beta_i$ , leaving the eigenvalues unchanged, any perturbation of the eigenvalues of  $\mathbf{H}_1$  must be even in  $\tilde{k}'$ , and thus the first

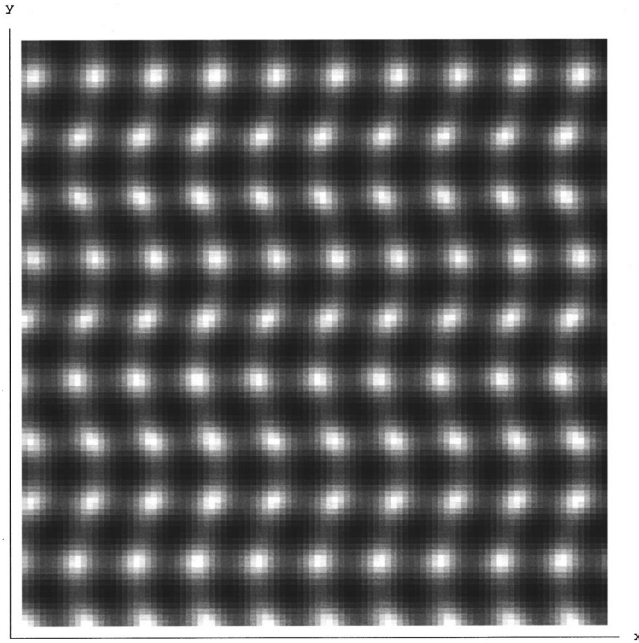


FIG. 2. The zigzag instability, shown by the same means as in Fig. 1. The displacements of the maxima are in the  $x$  direction, while the modulation wave vector  $\vec{k}'$  is in the  $y$  direction.

order perturbation vanishes identically. To perform second order perturbation theory on  $\mathbf{H}_1$  we first define the direction cosines for  $\vec{k}'$ ,

$$A \equiv \hat{k}_1 \cdot \vec{k}' / k', \quad B \equiv \hat{k}_2 \cdot \vec{k}' / k', \quad C \equiv \hat{k}_3 \cdot \vec{k}' / k'.$$

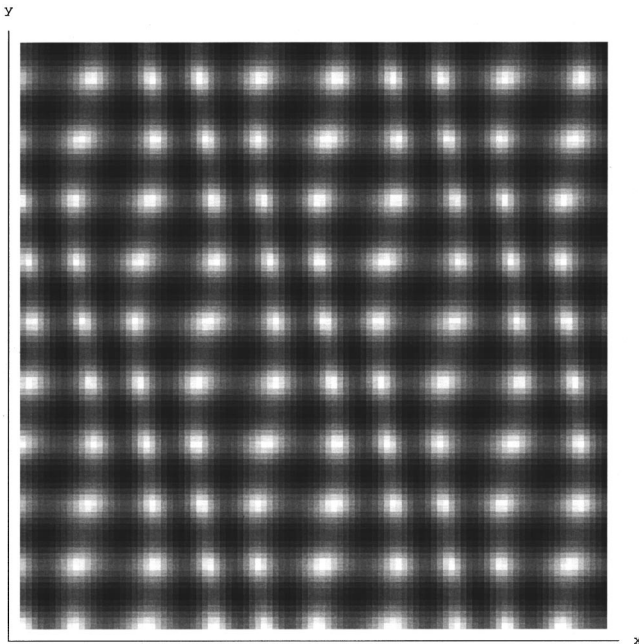


FIG. 3. The skew-varicose instability, shown by the same means as Figs. 1 and 2. The displacements of the maxima are in the  $x$  direction, but the modulation wave vector  $\vec{k}'$  is neither parallel nor perpendicular to them.

Then

$$\begin{aligned} & \langle \phi_l | \mathbf{H}_1 | \phi_i \rangle \Big|_{i=1,2,3}^{l=4,5,6} \\ &= 2\delta k' (\tilde{k}^2 - 1) \downarrow \begin{matrix} l \rightarrow \\ i \downarrow \end{matrix} \begin{pmatrix} A & A & A \\ -B & B & B \\ 0 & -2C & C \end{pmatrix} \\ & \text{(states not normalized).} \end{aligned}$$

If we normalize the states properly, we get the second order matrix (see Ref. [15])

$$\begin{aligned} \mathbf{V}_{ij} & \equiv \sum_{l=4}^6 \frac{\langle \phi_l | \mathbf{H}_1 | \phi_i \rangle \langle \phi_l | \mathbf{H}_1 | \phi_j \rangle}{-e_l} \\ &= -\delta^2 k'^2 (\tilde{k}^2 - 1)^2 \left\{ \frac{1}{6r^2 h_3} \begin{pmatrix} 2A^2 & -AB & -AC \\ -AB & 2B^2 & -BC \\ -AC & -BC & 2C^2 \end{pmatrix} \right. \\ & \quad \left. + \frac{1}{6r^2 (3h_{1,\sigma_1} + h_3)} \begin{pmatrix} A^2 & AB & AC \\ AB & B^2 & BC \\ AC & BC & C^2 \end{pmatrix} \right\}. \end{aligned}$$

The overall factor  $(\tilde{k}^2 - 1)^2$  is already  $O(q^2)$ . This expression is to be combined with the corresponding first order result for  $\mathbf{H}_2$ , which is of the same order as  $\mathbf{V}$ ,

$$\langle \phi_i | \mathbf{H}_2 | \phi_j \rangle \Big|_{i,j=1,2,3} = -\delta k'^2 \begin{pmatrix} A^2 & & \\ & B^2 & \\ & & C^2 \end{pmatrix}.$$

The result can be simplified using the expression

$$r^2 = \frac{\frac{1}{4} \delta (\tilde{k}^2 - 1)^2 - \lambda}{3h_{1,\sigma_1} + h_3} = \frac{\delta q^2 - \lambda}{3h_{1,\sigma_1} + h_3}$$

from Eq. (3.2), where we have used the substitution

$$\tilde{k} = \sqrt{1 + 2q}. \quad (3.7)$$

Thus  $q = \hat{k}_1 \cdot \vec{q}_1 + \frac{1}{2} |\vec{q}_1|^2$  (and likewise for  $i=2,3$ ) and this *new* variable absorbs all contributions from the second derivative in  $\square$ . For small  $q$  (or  $|\vec{q}_1|$ ) this is a well-defined, i.e., one-to-one, relationship between  $q$  and  $\tilde{k}$ . The eigenvalues of the resulting perturbation matrix  $\mathbf{V}_{ij} + \langle \phi_i | \mathbf{H}_2 | \phi_j \rangle$  are now  $\delta k'^2$  times the solutions in  $t$  to

$$t^3 + \Delta t^2 + \Xi t + \Upsilon = 0,$$

where

$$\Delta = \frac{(A^2 + B^2 + C^2)[\lambda - \Gamma_2 \delta q^2]}{\lambda - \delta q^2},$$

$$\Xi = \frac{(A^2B^2 + A^2C^2 + B^2C^2)[\lambda - \Gamma_1 \delta q^2][\lambda - \Gamma_3 \delta q^2]}{(\lambda - \delta q^2)^2},$$

$$Y = \frac{A^2B^2C^2(\lambda - 3\delta q^2)[\lambda - \Gamma_3 \delta q^2]^2}{(\lambda - \delta q^2)^3},$$

and

$$\Gamma_1 \equiv \frac{3h_3 + 2h_{1,\sigma_1}}{h_3} > 0, \quad \Gamma_2 \equiv \frac{3h_3 + 4h_{1,\sigma_1}}{h_3} > 0,$$

$$\Gamma_3 \equiv \frac{3h_3 + 6h_{1,\sigma_1}}{h_3} > 0.$$

Note that, if we use Eq. (3.5), then

$$\begin{aligned} h_{1,\sigma_1} < 0 &\Rightarrow 3 < \Gamma_1 < \Gamma_2 < \Gamma_3, \\ h_{1,\sigma_1} > 0 &\Rightarrow 3 > \Gamma_1 > \Gamma_2 > \Gamma_3. \end{aligned} \quad (3.8)$$

The simple-cubic pattern is stable (with respect to long-wavelength instabilities) if the three eigenvalues have a negative real part for all values of  $A$ ,  $B$ , and  $C$ , which requires  $\Delta$ ,  $\Xi$ , and  $Y$  all to be positive. Since the denominators are already positive, we need only examine the numerators. We examine first the possibility that  $Y$  passes through 0 becoming negative and triggering an instability. This occurs for

$$\lambda < 3\delta q^2.$$

The inequalities (3.8) indicate that this condition provides the stability limit when  $h_{1,\sigma_1} > 0$ . To interpret the nature of this instability we substitute  $\lambda = 3\delta q^2$  into  $\mathbf{V}_{ij} + \langle \phi_i | \mathbf{H}_2 | \phi_j \rangle$  and find that the null eigenvector is of the form  $(BC, AC, AB)$ , which in the original  $\xi$  basis is  $BC|\phi_1\rangle + AC|\phi_2\rangle + AB|\phi_3\rangle$ . This is therefore a general skew-varicose instability, with wave vector  $\vec{k}'$  pointing in the direction  $(A, B, C)$ , but the maxima shifted in the direction  $(BC, AC, AB)$ . It can, however, be a zigzag instability if  $ABC = 0$ , or an Eckhaus instability if  $A^2 = B^2 = C^2 = \frac{1}{3}$ . The case  $A = 0$  (or  $B = 0$  or  $C = 0$ ) is special because the calculation must be carried to next order in perturbation theory in order to determine stability. We postpone this calculation.

When  $h_{1,\sigma_1} < 0$  the corresponding stability boundary is given by  $\lambda = \Gamma_3 \delta q^2$ . Along this curve both  $Y$  and  $\Xi$  vanish and there is therefore a double zero eigenvalue. Moreover,  $\Xi$  also passes through zero along the curve  $\lambda = \Gamma_1 \delta q^2$ . The system is thus also unstable ( $\Xi < 0$ ) when

$$\Gamma_1 < \lambda / \delta q^2 < \Gamma_3 \quad \text{for } h_{1,\sigma_1} < 0,$$

$$\Gamma_1 > \lambda / \delta q^2 > \Gamma_3 \quad \text{for } h_{1,\sigma_1} > 0.$$

Since the two null eigenvectors when  $\lambda = \Gamma_3 \delta q^2$  are  $(B, -A, 0)$  and  $(C, 0, -A)$  and these span the plane perpendicu-

lar to the modulation wave vector  $\vec{k}' = (A, B, C)$ , this instability corresponds to a zigzag instability.

The remaining possibility for instability, that  $\Delta < 0$ , occurs for  $\lambda / \delta q^2 < \Gamma_2$ , but in view of (3.8) this condition does not introduce any new stability boundaries. The condition becomes important, however, when  $h_{1,\sigma_1} < 0$  because it implies that the simple-cubic pattern will be unstable for all  $\lambda < \Gamma_3 \delta q^2$ , i.e., that the pattern is also unstable in the interval  $3\delta q^2 < \lambda < \Gamma_1 \delta q^2$ .

We still have to deal with the case  $A = 0$ . In this case  $Y$  vanishes identically to this order in perturbation theory. To determine whether or not it actually passes through 0, we look at terms that are  $O(qk'^2)$ . We get no such term from  $\mathbf{H}_1$ , whereas to the order we desire,

$$\begin{aligned} \langle \phi_i | \mathbf{H}_2 | \phi_j \rangle |_{i,j=1,2,3} &= -k'^2 \delta \begin{pmatrix} 0 & & \\ & B^2 & \\ & & C^2 \end{pmatrix} \\ &- 2k' \delta \begin{pmatrix} 0 & & \\ & B(\vec{q}_2 \cdot \vec{k}') & \\ & & C(\vec{q}_3 \cdot \vec{k}') \end{pmatrix} \end{aligned}$$

and

$$\langle \phi_i | \mathbf{H}_3 | \phi_j \rangle = -\delta q k'^2 \mathbf{1}.$$

Our new perturbation matrix is

$$\begin{aligned} &\mathbf{V}_{ij} + \langle \phi_i | \mathbf{H}_2 | \phi_j \rangle + \langle \phi_i | \mathbf{H}_3 | \phi_j \rangle \\ &= (\mathbf{V}_{ij} + \langle \phi_i | \mathbf{H}_2 | \phi_j \rangle)_{\text{old}} + \tilde{\mathbf{H}} \\ &= (\mathbf{V}_{ij} + \langle \phi_i | \mathbf{H}_2 | \phi_j \rangle)_{\text{old}} \\ &- 2k' \delta \begin{pmatrix} 0 & & \\ & B(\vec{q}_2 \cdot \vec{k}') & \\ & & C(\vec{q}_3 \cdot \vec{k}') \end{pmatrix} - \delta q k'^2 \mathbf{1}. \end{aligned}$$

We calculate the new eigenvalue by using perturbation theory upon our previous perturbation results. That is, we wish to find corrections to the 0 eigenvalue of the matrix  $(\mathbf{V}_{ij} + \langle \phi_i | \mathbf{H}_2 | \phi_j \rangle)_{\text{old}}$  for the case  $A = 0$ . We assume first that this eigenvalue is nondegenerate. Then the null eigenvector is  $\langle \phi_1 | = (1, 0, 0)$  and

$$\langle \phi_1 | \tilde{\mathbf{H}} | \phi_1 \rangle = -\delta q k'^2.$$

Thus for  $q < 0$  there exists a  $\vec{k}'$  that makes our system unstable. Furthermore, if  $A = 0$ , then  $\vec{k}'$  is in the  $y$ - $z$  plane, but the unstable eigenvector is  $|\phi_1\rangle$  so the shifts are in the  $x$  direction. Thus this is a zigzag instability. To check for possible multiple 0 eigenvalues we set  $A = 0$  and compute the determinant of the nonvanishing  $2 \times 2$  submatrix of  $(\mathbf{V}_{ij} + \langle \phi_i | \mathbf{H}_2 | \phi_j \rangle)_{\text{old}}$ ,

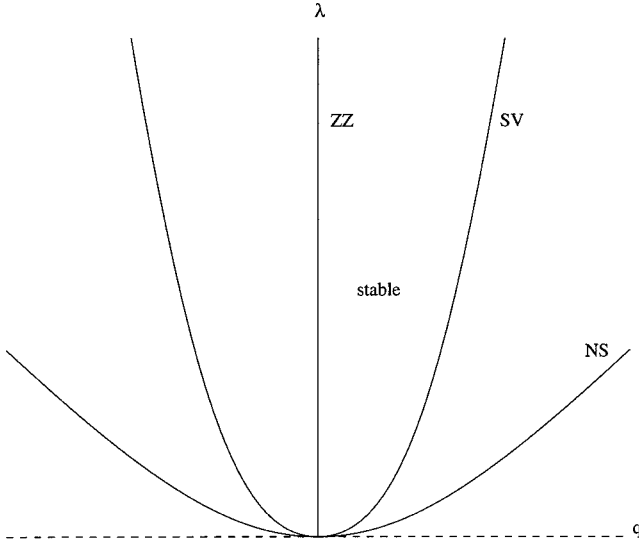


FIG. 4. The lower portion of the Busse balloon for the sc solution, showing the neutral stability (NS), skew-varicose (SV), and zigzag (ZZ) boundaries and the resulting region of stability. The SV boundary is present when  $h_{1,\sigma_1} > 0$ , and is replaced by another zigzag boundary when  $h_{1,\sigma_1} < 0$ .

$$\frac{B^2 C^2 \delta^2 [\lambda - \Gamma_1 \delta q^2] [\lambda - \Gamma_3 \delta q^2]}{(\lambda - \delta q^2)^2} k'^4.$$

The instabilities due to the  $\lambda$ -dependent terms in the numerator have already been described. The only remaining possibilities for finding a multiple zero eigenvalue are  $B=0$  and  $C=0$ . For example, if  $A=B=0$  (and hence  $C=1$ ) there are two independent null eigenvectors spanning the  $x$ - $y$  plane while  $\vec{k}'$  is in the  $z$  direction, again corresponding to a zigzag instability. We summarize the above results in Fig. 4.

It is worth noting that the substitution (3.7), namely,  $\tilde{k} = \sqrt{1+2q}$  implies

$$(\tilde{k}^2 - 1)^2 = 4q^2 = [2(\hat{k}_1 \cdot \vec{q}_1)^2 + |\vec{q}_1|^2]^2.$$

Consequently we may think of  $q$  as the magnitude  $\hat{k}_1 \cdot \vec{q}_1$  and Eq. (3.7) as an *approximation* instead of a substitution introducing a new variable. This approximation is equivalent to neglecting the higher order term  $-(i/2)\nabla^2$  in  $\square_1$ . Thus the only difference between the calculation with isotropy-preserving terms and without lies in the near-identity relationship between  $q$  and  $\hat{k}_1 \cdot \vec{q}_1$ . The stability diagrams calculated in these two ways therefore differ only by a near-identity rescaling of the horizontal axis. This is an example of a general result that the use of  $\square$  does not affect the stability properties of *periodic* solutions, at least in the limit of long-wavelength perturbations [14].

### B. The lamellas

To study the stability of lamellas on the sc lattice, we assume  $r_1=r$ ,  $r_2=r_3=0$ . We again restrict ourselves to a

subset of all possible distortions of the lattice. The equilibrium condition (3.2), in the limit of small  $z_2$  and  $z_3$ , yields the two conditions

$$\lambda + (h_{1,\sigma_1} + h_3)r^2 = \frac{1}{4}\delta(\tilde{k}_1^2 - 1)^2 + O(q^3, r^3) \quad (3.9)$$

and

$$h_3 r^2 = \frac{1}{4}\delta(\tilde{k}_1^2 - 1)^2 - \frac{1}{4}\delta(\tilde{k}_2^2 - 1)^2, \quad \tilde{k}_2^2 = \tilde{k}_3^2.$$

The latter appears to provide a restriction on the allowed distortion of the sc lattice. In fact, an examination of the calculation that follows shows readily that none of the stability results depend on this restriction, i.e., the results apply to strictly one-dimensional structures (lamellas). The additional equations are retained purely for convenience so that all the problems analyzed have the same algebraic structure and can therefore be solved by an identical method. In the present case we find that the new lowest order matrix is

$$\mathbf{H}_0 = r^2 \begin{pmatrix} \mathbf{P} & & & & & \\ & \mathbf{Q} & & & & \\ & & \mathbf{Q} & & & \\ & & & & & \\ & & & & & \\ & & & & & \end{pmatrix}, \quad \mathbf{P} = (h_{1,\sigma_1} + h_3) \begin{pmatrix} 1 & 1 \\ 1 & 1 \end{pmatrix},$$

$$\mathbf{Q} = -h_3 \begin{pmatrix} 1 & \\ & 1 \end{pmatrix}.$$

The (orthogonal) eigenvectors are the columns of

$$\Phi = (\phi_1, \dots, \phi_6) = \begin{pmatrix} 1 & 1 & 0 & 0 & 0 & 0 \\ -1 & 1 & 0 & 0 & 0 & 0 \\ 0 & 0 & 1 & 0 & 0 & 0 \\ 0 & 0 & 0 & 1 & 0 & 0 \\ 0 & 0 & 0 & 0 & 1 & 0 \\ 0 & 0 & 0 & 0 & 0 & 1 \end{pmatrix},$$

and correspond to the eigenvalues

$$\{e_i\}_{i=1,\dots,6} = r^2 \{0, 2(h_{1,\sigma_1} + h_3), -h_3, -h_3, -h_3, -h_3\},$$

respectively. Thus only the first eigenvalue can trigger a long-wavelength instability. Note, in particular, that the last four eigenvalues are stable (if  $h_3 > 0$ ) indicating that the constraints in Eq. (3.9) play no role. As before, the first order perturbation calculation for  $\mathbf{H}_1$  does not contribute, while  $\mathbf{H}_2$  yields

$$\langle \phi_1 | \mathbf{H}_2 | \phi_1 \rangle = -\delta k'^2 A^2.$$

For the normalized second order calculation for  $\mathbf{H}_1$  we first note that

$$\langle \phi_l | \mathbf{H}_1 | \phi_l \rangle |_{l=2,\dots,6} = \delta k' (\tilde{k}_1^2 - 1) (-A \quad 0 \quad 0 \quad 0 \quad 0)$$

and then calculate the second order contribution as for the sc pattern. The combined result is the  $1 \times 1$  matrix

TABLE II. Maximal isotropy branches for the fcc lattice.

Name	Solution	$\sigma_1$	Branching equation
Trivial	(0,0,0,0)	0	$\sigma_1 = 0$
Lamellas	(x,0,0,0)	$x^2$	$\lambda + (h_{1,\sigma_1} + h_3)\sigma_1 = 0$
Rhombic prisms	(x,x,0,0)	$2x^2$	$\lambda + \frac{1}{2}(2h_{1,\sigma_1} + h_3)\sigma_1 = 0$
fcc	(x,x,x,x)	$4x^2$	$\lambda + \frac{1}{4}(4h_{1,\sigma_1} + h_3 + p_3)\sigma_1 = 0$
Double diamond	(-x,x,x,x)	$4x^2$	$\lambda + \frac{1}{4}(4h_{1,\sigma_1} + h_3 - p_3)\sigma_1 = 0$

$$\mathbf{V}_{ij} + \langle \phi_i | \mathbf{H}_2 | \phi_j \rangle = - \frac{\delta^2 k'^2 (\tilde{k}_1^2 - 1)^2}{2(h_{1,\sigma_1} + h_3)r^2} A^2 - \delta k'^2 A^2.$$

As before, we use the substitution  $\tilde{k}_1 = \sqrt{1 + 2q}$ , which transforms this result into

$$\mathbf{V}_{ij} = \langle \phi_i | \mathbf{H}_2 | \phi_j \rangle = - \frac{\lambda - 3\delta q^2}{\lambda - \delta q^2} \delta k'^2 A^2.$$

If  $A \neq 0$  then for  $\lambda < 3\delta q^2$  the lamellas are unstable to  $|\phi_1\rangle$ . This eigenvector corresponds to a shift of the maxima in the  $x$  direction. When  $0 < A < 1$  this is a skew-varicose instability, and is independent of the perturbation wave vector  $\vec{k}'$ . In the  $q$ - $\lambda$  plane this degeneracy manifests itself in the fact that the stability boundary is identical for every direction of  $\vec{k}'$ . The retention of terms of higher order in  $q$  resolves the degeneracy and separates the stability boundaries for the different  $\vec{k}'$ . With these higher order terms, the stability boundary in the  $q$ - $\lambda$  plane for  $A$  away from 0 is given by

$$\lambda = 3\delta q^2 - \frac{2\delta q^3}{A^2} + O(q^4),$$

showing that instability first sets in at  $A = 1$ ; this is the Eckhaus instability.

The degeneracy can also be resolved by the NWS approach. In fact, these two approaches differ only in their truncations, with Gunaratne's truncation reducing to the NWS amplitude equation at leading order in  $q$ . The latter approach leads to a similar expression for the stability boundary,

$$\lambda = 3\delta q^2 - \delta q^3 - \frac{2\delta q^3}{A^2} + O(q^4),$$

where  $q = q_1 + \frac{1}{2}q_1^2$  is still given by Eq. (3.7). The difference between these two expressions is due to a difference at higher order in the approximation to the neutral stability curve, but contributes only a small overall shift of the stability boundary. In particular, the instability that first sets in is still of Eckhaus type.

If  $A = 0 \neq B, C$ ,  $\vec{k}'$  is perpendicular to  $\hat{k}_1$  and the same calculation as for the sc solution shows that the contribution from  $O(qk'^2)$  terms is

$$\langle \phi_1 | \tilde{\mathbf{H}} | \phi_1 \rangle = \langle \phi_1 | \mathbf{H}_3 | \phi_1 \rangle = -\delta q k'^2.$$

A zigzag instability is therefore present for  $q < 0$ . Note that since  $|q| \ll 1$  the growth rate of this instability is *slower* than that of the Eckhaus instability computed above.

#### IV. THE FCC LATTICE

The analysis of the stability properties of periodic patterns on the fcc lattice is similar to that performed for the sc lattice. Such patterns are generated by the vectors  $\pm \hat{k}_i$ , where

$$\hat{k}_1 = (\hat{x} - \hat{y} - \hat{z})/\sqrt{3}, \quad \hat{k}_2 = (-\hat{x} + \hat{y} - \hat{z})/\sqrt{3},$$

$$\hat{k}_3 = (-\hat{x} - \hat{y} + \hat{z})/\sqrt{3}, \quad \hat{k}_4 = (\hat{x} + \hat{y} + \hat{z})/\sqrt{3}.$$

The resulting amplitude equations take the form [6]

$$\begin{aligned} \dot{z}_1 = & \lambda z_1 + (h_{1,\sigma_1} + h_3)|z_1|^2 z_1 + h_{1,\sigma_1}(|z_2|^2 + |z_3|^2 + |z_4|^2)z_1 \\ & + p_3 \bar{z}_2 \bar{z}_3 \bar{z}_4 + \delta \square_1^2 z_1 + O(\square^4, \mathbf{z}^4) \end{aligned}$$

with three other equations obtained by cyclic permutation. The possible maximal steady states on this lattice are summarized in Table II. As in the sc case we consider long-wavelength instabilities of only the potentially stable patterns, i.e., the fcc and double diamond (dd) patterns, as well as lamellas [6].

##### A. The fcc and dd solutions

The fcc solution is the solution with  $r_i = r$ ,  $i = 1, 2, 3, 4$ . The results for the dd solution can be obtained by changing  $p_3 \rightarrow -p_3$  in what follows, and are therefore not listed separately. We consider the stability of equilibria of the form

$$\lambda + (4h_{1,\sigma_1} + h_3 + p_3)r^2 = \frac{1}{4}\delta(\tilde{k}_i^2 - 1)^2 + O(q^3, r^3)$$

and require the  $\tilde{k}_i^2$  to be the same for every  $i$ . The evolution equation for the perturbation  $\alpha_1$  is now

$$\begin{aligned} \dot{\alpha}_1 = & r^2[(h_{1,\sigma_1} + h_3)(\alpha_1 + \beta_1) + h_{1,\sigma_1}(\alpha_2 + \beta_2 + \alpha_3 + \beta_3 + \alpha_4 \\ & + \beta_4) + p_3(\beta_2 + \beta_3 + \beta_4 - \alpha_1)] - \delta\alpha_1[(\tilde{k}_1^2 - 1)(\tilde{k}_1 \cdot \vec{k}') \\ & + (\tilde{k}_1 \cdot \vec{k}')^2 + \frac{1}{2}(\tilde{k}_1^2 - 1)k'^2] + O(k'^3; q^3, r^3). \end{aligned}$$

The corresponding result for  $\beta_1$  is obtained by changing the sign of  $\vec{k}'$  and interchanging  $\alpha_i$  and  $\beta_i$ , etc. These equations yield the  $4 \times 4$  matrices

$$\mathbf{H}_0 = r^2 \begin{pmatrix} \mathbf{P} & \mathbf{Q} & \mathbf{Q} & \mathbf{Q} \\ \mathbf{Q} & \mathbf{P} & \mathbf{Q} & \mathbf{Q} \\ \mathbf{Q} & \mathbf{Q} & \mathbf{P} & \mathbf{Q} \\ \mathbf{Q} & \mathbf{Q} & \mathbf{Q} & \mathbf{P} \end{pmatrix},$$

$$\mathbf{P} = (h_{1,\sigma_1} + h_3) \begin{pmatrix} 1 & 1 \\ 1 & 1 \end{pmatrix} - p_3 \begin{pmatrix} 1 & 0 \\ 0 & 1 \end{pmatrix},$$

$$\mathbf{Q} = h_{1,\sigma_1} \begin{pmatrix} 1 & 1 \\ 1 & 1 \end{pmatrix} + p_3 \begin{pmatrix} 0 & 1 \\ 1 & 0 \end{pmatrix},$$

$$\mathbf{H}_1 = -\delta(\tilde{k}^2 - 1) \begin{pmatrix} \mathbf{K}_1 & & & \\ & \mathbf{K}_2 & & \\ & & \mathbf{K}_3 & \\ & & & \mathbf{K}_4 \end{pmatrix},$$

$$\mathbf{K}_j = (\tilde{k}_j \cdot \tilde{k}') \begin{pmatrix} 1 & \\ & -1 \end{pmatrix},$$

$$\mathbf{H}_2 = -\delta \begin{pmatrix} \mathbf{K}_1^2 & & & \\ & \mathbf{K}_2^2 & & \\ & & \mathbf{K}_3^2 & \\ & & & \mathbf{K}_4^2 \end{pmatrix},$$

$$\mathbf{H}_3 = -\frac{\delta}{2}(\tilde{k}^2 - 1)k'^2 \mathbf{1}.$$

The (orthonormal) eigenvectors of  $\mathbf{H}_0$  are now the columns of

$$\Phi = (\phi_1, \dots, \phi_8)$$

$$= \frac{1}{2\sqrt{2}} \begin{pmatrix} 1 & -1 & -1 & 1 & 1 & -1 & -1 & 1 \\ -1 & 1 & 1 & -1 & 1 & -1 & -1 & 1 \\ -1 & 1 & -1 & 1 & -1 & 1 & -1 & 1 \\ 1 & -1 & 1 & -1 & -1 & 1 & -1 & 1 \\ -1 & -1 & 1 & 1 & -1 & -1 & 1 & 1 \\ 1 & 1 & -1 & -1 & -1 & -1 & 1 & 1 \\ 1 & 1 & 1 & 1 & 1 & 1 & 1 & 1 \\ -1 & -1 & -1 & -1 & 1 & 1 & 1 & 1 \end{pmatrix}$$

and correspond to the eigenvalues

$$\{e_i\}_{i=1, \dots, 8} = r^2 \{0, 0, 0, -4p_3, \underbrace{2(h_3 - p_3)}_{\text{thrice}}, 2(4h_{1,\sigma_1} + h_3 + p_3)\},$$

respectively. The first four eigenvectors are PM modes and the last four are AM modes. The undistorted fcc state is therefore stable, provided

$$p_3 > 0, \quad h_3 - p_3 < 0, \quad 4h_{1,\sigma_1} + h_3 + p_3 < 0, \quad (4.1)$$

and we assume henceforth that these conditions hold.

The three null eigenvectors  $|\phi_1\rangle$ ,  $|\phi_2\rangle$ , and  $|\phi_3\rangle$  represent shifts in the  $x$ ,  $y$ , and  $z$  directions, respectively, and these

can all lead to long-wavelength instabilities. To calculate the corrections to the corresponding zero eigenvalues we need, as before, to go to second order in perturbation theory. We define  $A$ ,  $B$ , and  $C$  as before and include

$$D \equiv \hat{k}_4 \cdot \tilde{k}' / k'.$$

Then

$$\langle \phi_i | \mathbf{H}_1 | \phi_i \rangle \Big|_{i=4, \dots, 8}^{i=1,2,3} = \frac{\delta}{4} k' (\tilde{k}^2 - 1) \begin{matrix} l \rightarrow \\ \downarrow \end{matrix} \begin{pmatrix} 0 & 0 & 0 \\ -A - B - C - D & A + B - C - D & A - B + C - D \\ A + B - C - D & -A - B - C - D & -A + B + C - D \\ A - B + C - D & -A + B + C - D & -A - B - C - D \\ -A + B + C - D & A - B + C - D & A + B - C - D \end{pmatrix}. \quad (4.2)$$

The eigenvector  $\langle \phi_4 |$  plays no role and we delete it in the sequel. By construction,  $\mathbf{H}_1$  rotates PM modes into AM modes and vice versa. Thus the second order perturbation of the null PM eigenmodes can only contain cross terms involving AM modes.

Since  $A + B + C + D = 0$ , the result (4.2) reduces to

$$\langle \phi_l | \mathbf{H}_1 | \phi_i \rangle \Big|_{l=5, \dots, 8}^{i=1, 2, 3} = \frac{\delta}{2} k' (\tilde{k}^2 - 1) \times \begin{matrix} i \rightarrow \\ \downarrow l \\ \begin{pmatrix} 0 & A+B & A+C \\ A+B & 0 & B+C \\ A+C & B+C & 0 \\ B+C & A+C & A+B \end{pmatrix} \end{matrix}.$$

We now define

$$A + B \equiv -2Z/\sqrt{3}, \quad A + C \equiv -2Y/\sqrt{3}, \quad B + C \equiv -2X/\sqrt{3},$$

so that

$$X = \hat{x} \cdot \tilde{k}' / k', \quad Y = \hat{y} \cdot \tilde{k}' / k', \quad Z = \hat{z} \cdot \tilde{k}' / k'$$

and

$$X^2 + Y^2 + Z^2 = 1. \quad (4.3)$$

These are again the direction cosines of  $\tilde{k}'$ . It follows that

$$\langle \phi_l | \mathbf{H}_1 | \phi_i \rangle \Big|_{l=5, \dots, 8}^{i=1, 2, 3} = -\frac{\delta}{\sqrt{3}} k' (\tilde{k}^2 - 1) \begin{pmatrix} 0 & Z & Y \\ Z & 0 & X \\ Y & X & 0 \\ X & Y & Z \end{pmatrix}$$

so that

$$\mathbf{V}_{ij} \equiv \sum_{l=5}^8 \frac{\langle \phi_l | \mathbf{H}_1 | \phi_i \rangle \langle \phi_l | \mathbf{H}_1 | \phi_j \rangle}{-e_l} = -\delta^2 k'^2 (\tilde{k}^2 - 1)^2 \times \left\{ \frac{1}{6r^2(h_3 - p_3)} \begin{pmatrix} Y^2 + Z^2 & XY & XZ \\ XY & X^2 + Z^2 & YZ \\ XZ & YZ & X^2 + Y^2 \end{pmatrix} + \frac{1}{6r^2(4h_{1,\sigma_1} + h_3 + p_3)} \begin{pmatrix} X^2 & XY & XZ \\ XY & Y^2 & YZ \\ XZ & YZ & Z^2 \end{pmatrix} \right\}.$$

To this result we add the first order contribution from  $\mathbf{H}_2$ ,

$$\langle \phi_i | \mathbf{H}_2 | \phi_j \rangle = -\frac{\delta}{3} k'^2 \begin{pmatrix} X^2 + Y^2 + Z^2 & 2XY & 2XZ \\ 2XY & X^2 + Y^2 + Z^2 & 2YZ \\ 2XZ & 2YZ & X^2 + Y^2 + Z^2 \end{pmatrix}.$$

We now proceed as in the sc case and express the total perturbation matrix  $\mathbf{V}_{ij} + \langle \phi_i | \mathbf{H}_2 | \phi_j \rangle$  in terms of  $q$  instead of  $\tilde{k}$  and eliminate  $r^2$ . The eigenvalues are  $\delta k'^2$  times the solutions in  $t$  to

$$t^3 + \Delta t^2 + \Xi t + Y = 0,$$

where

$$\Delta = \frac{\lambda - \Gamma_1 \delta q^2}{\lambda - \delta q^2}, \quad \Xi = \frac{(\lambda - \Gamma_2 \delta q^2) N_{\Xi}}{9(p_3 - h_3)(\lambda - \delta q^2)^2},$$

$$Y = \frac{[\lambda - \Gamma_2 \delta q^2]^2 N_Y}{27(p_3 - h_3)(\lambda - \delta q^2)^3}.$$

Here

$$\Gamma_1 = 3 + \frac{8}{3} \eta, \quad \Gamma_2 = 3 + 4 \eta,$$

where

$$\eta \equiv -\frac{2h_{1,\sigma_1} + p_3}{p_3 - h_3}$$

[the inequalities (4.1) guarantee that  $\eta > -\frac{1}{2}$ ], while

$$N_{\Xi} = (p_3 - h_3)(3 - 4X^2 + 4X^4 - 4Y^2 + 4X^2Y^2 + 4Y^4)\lambda + (8h_{1,\sigma_1} + 9h_3 - 5p_3 - 12h_3X^2 + 12p_3X^2 + 12h_3X^4 - 12p_3X^4 - 12h_3Y^2 + 12p_3Y^2 + 12h_3X^2Y^2 - 12p_3X^2Y^2 + 12h_3Y^4 - 12p_3Y^4) \delta q^2 \quad (4.4)$$

and

$$N_Y = (p_3 - h_3)(1 - 4X^2 + 4X^4 - 4Y^2 + 20X^2Y^2 - 16X^4Y^2 + 4Y^4 - 16X^2Y^4)\lambda + (3h_3 - 3p_3 - 12h_3X^2 + 12p_3X^2 + 12h_3X^4 - 12p_3X^4 - 12h_3Y^2 + 12p_3Y^2 + 32h_{1,\sigma_1}X^2Y^2 + 60h_3X^2Y^2 - 44p_3X^2Y^2 - 32h_{1,\sigma_1}X^4Y^2 - 48h_3X^4Y^2 + 32p_3X^4Y^2 + 12h_3Y^4 - 12p_3Y^4 - 32h_{1,\sigma_1}X^2Y^4 - 48h_3X^2Y^4 + 32p_3X^2Y^4) \delta q^2. \quad (4.5)$$

In writing these expressions we have eliminated  $Z$  using Eq. (4.3).

The symmetry of the perturbation matrix guarantees that all the eigenvalues are real. They are all negative if and only if  $\Delta$ ,  $\Xi$ , and  $Y$  are all positive. Consequently instability only arises when an eigenvalue (or two or three) passes through 0, i.e., the condition  $Y = 0$  is a necessary condition for the appearance of (long-wavelength) instability. Nevertheless, it is helpful to look first at the coefficient  $\Delta$ . In view of the inequalities (4.1) and the requirement  $\lambda > \delta q^2$ , the coefficient  $\Delta < 0$  if and only if

$$\lambda/\delta q^2 < \Gamma_1.$$

Moreover,  $\Xi$  has a single zero and  $Y$  a double zero at

$$\lambda/\delta q^2 = \Gamma_2$$

and instability occurs for  $\lambda/\delta q^2 \leq \Gamma_2$  if  $N_\Xi \geq 0$ . The quantity  $N_\Xi = 0$  when  $\lambda/\delta q^2 = \Gamma_\Xi(X, Y)$ , a quantity readily obtained from Eq. (4.4).

To establish the conditions for instability we need to determine, for given  $h_{1,\sigma_1}$ ,  $h_3$ , and  $p_3$ , the maximum and minimum of  $\Gamma_\Xi(X, Y)$  over all directions of  $\vec{k}'$ , i.e., on the domain  $X^2 + Y^2 \leq 1$ . The result is

$$\text{extrema } \Gamma_\Xi(X, Y) = \left\{ 3 + \frac{4}{3}\eta, 3 + \frac{12}{5}\eta \right\} \equiv \{ \Gamma_{\Xi,1}, \Gamma_{\Xi,2} \}.$$

$X^2 + Y^2 \leq 1$

Similarly, for each direction of  $\vec{k}'$ ,  $Y = 0$  at  $\lambda/\delta q^2 = \Gamma_Y(X, Y)$ , a quantity obtained from Eq. (4.5). The extrema on the domain  $X^2 + Y^2 \leq 1$  are

$$\text{extrema } \Gamma_Y(X, Y) = \left\{ 3, 3 + \frac{16}{7}\eta \right\};$$

$X^2 + Y^2 \leq 1$

we denote the second of these by  $\Gamma_Y$ . Thus for  $\eta > 0$ ,

$$3 < \Gamma_{\Xi,1} < \Gamma_Y < \Gamma_{\Xi,2} < \Gamma_1 < \Gamma_2.$$

For  $\eta < 0$  the order is reversed, in which case the lower bound on  $\eta$  guarantees that  $\Gamma_2 > 1$ .

In view of the above results the fcc state is stable with respect to long-wavelength instabilities if and only if  $\lambda/\delta q^2 > \max\{\Gamma_2, 3\}$ . As  $\lambda$  passes through  $\Gamma_2 \delta q^2$  two eigenvalues pass through 0 for every wave vector  $\vec{k}'$ . The corresponding null eigenvectors, obtained from  $\mathbf{V}_{ij} + \langle \phi_i | \mathbf{H}_2 | \phi_j \rangle$ , are  $(Y, -X, 0)$  and  $(Z, 0, -X)$ . These span the subspace perpendicular to  $(X, Y, Z)$  and indicate that the instability is a zigzag instability with no preference for a particular wave vector  $\vec{k}'$  and no preference for a particular ‘‘polarization.’’

As  $\lambda$  passes through  $3 \delta q^2$  only certain wave vectors produce unstable eigenvalues. Since  $\Gamma_Y = 3$  only for  $XYZ = 0$  we assume without loss of generality that  $Z = 0$ , so that  $\vec{k}'$  lies in the  $x$ - $y$  plane. Substitution of both  $Z = 0$  and  $\lambda = 3 \delta q^2$  into  $\mathbf{V}_{ij} + \langle \phi_i | \mathbf{H}_2 | \phi_j \rangle$  yields the null eigenvector  $(-X, Y, 0)$ . Since this vector is in general neither parallel nor perpendicular to  $\vec{k}'$ , the instability triggered at  $\lambda = 3 \delta q^2$  is in general a skew-varicose instability. However, if  $\vec{k}'$  points along a coordinate axis, the instability becomes an Eckhaus instability, while if it points midway between two axes the instability is a zigzag instability. Note that there is no need to go to higher order in perturbation theory, and that there is therefore no zigzag instability boundary at  $q = 0$ .

The stability properties of the lamellas on the fcc lattice with respect to long-wavelength perturbations are identical to those for the lamellas on the sc lattice.

## V. THE BCC LATTICE

Patterns with the symmetry of the bcc lattice are generated by the 12 wave vectors  $\pm \hat{k}_i$ , where

$$\hat{k}_1 = \frac{1}{\sqrt{2}}(1, 1, 0), \quad \hat{k}_2 = \frac{1}{\sqrt{2}}(0, 1, 1), \quad \hat{k}_3 = \frac{1}{\sqrt{2}}(1, 0, 1),$$

$$\hat{k}_4 = \frac{1}{\sqrt{2}}(1, -1, 0), \quad \hat{k}_5 = \frac{1}{\sqrt{2}}(0, 1, -1), \quad \hat{k}_6 = \frac{1}{\sqrt{2}}(-1, 0, 1).$$

Symmetry arguments lead to the (truncated) amplitude equations [7]

$$\begin{aligned} \dot{z}_1 = & \lambda z_1 + \frac{1}{2} a_{12} (z_2 \bar{z}_6 + z_3 \bar{z}_5) + a_1 |z_1|^2 z_1 + \frac{1}{4} a_3 (|z_2|^2 + |z_3|^2 \\ & + |z_5|^2 + |z_6|^2) z_1 + a_8 |z_4|^2 z_1 + \frac{1}{2} a_{16} (z_2 z_4 z_5 + z_3 \bar{z}_4 \bar{z}_6) \\ & + \delta \square_1^2 z_1 + O(\square^4, \mathbf{z}^4) \end{aligned} \quad (5.1)$$

with the remaining equations generated by the symmetries of the lattice. Since the quadratic equivariant renders all solutions unstable near onset we focus, following Ref. [7], on the case  $a_{12} \approx 0$  corresponding to a system with a weakly broken additional symmetry  $\mathbf{z} \rightarrow -\mathbf{z}$ . This assumption allows us to drop any even terms in  $\mathbf{z}$  allowed by symmetry involving  $\square$  [17], since the coefficients of these terms must also be expected to be  $O(a_{12})$ . When these terms are present but are small, their main effect is to introduce a slight asymmetry with respect to  $q = 0$  in the stability regions computed below. The possible primary solution branches when this additional symmetry is exact are listed in Table III. In the presence of small but nonzero  $a_{12}$  only six of these branches remain primary. The branches of lamellas, squares, bccI, and the solution  $A$  remain completely unaffected by this symmetry-breaking term, while the hexagonal prisms and bcc states now bifurcate in transcritical bifurcations. The remaining branches become secondary as detailed in Ref. [7].

In physical models the requirement that  $a_{12} \ll |a_1|$  may introduce constraints on the remaining coefficients. This is so in particular for general two-species reaction-diffusion models. These models have a special structure as a consequence of the law of mass action and as a result their bifurcation properties are a function of a single parameter. When this parameter is chosen so that  $a_{12} \ll 1$  the remaining coefficients have the fixed ratio

$$a_1 : a_3 : a_8 : a_{16} :: -1 : -8 : -2 : -4 \quad (5.2)$$

to leading order [18]. Motivated by this example we perform detailed Busse balloon computations only for this choice of coefficients. This choice restricts us to the study of long-wavelength instabilities of four states—bcc, bccI, lamellas, and hexagonal prisms—as we now describe.

### A. The solution bcc

We begin with the bcc solution, for which  $r_i = r$ ,  $i = 1, \dots, 6$ . The distorted equilibrium is given by

TABLE III. Maximal isotropy branches for the bcc lattice with the extra  $\mathbf{z} \rightarrow -\mathbf{z}$  symmetry.

Name	Solution	$\sigma_1$	Branching equation
Trivial	(0,0,0,0,0)	0	$\sigma_1=0$
Lamellas	(x,0,0,0,0)	$x^2$	$\lambda+a_1\sigma_1=0$
Rhombs	(x,x,0,0,0)	$2x^2$	$\lambda+\frac{1}{8}(4a_1+a_3)\sigma_1=0$
Squares	(x,0,0,x,0)	$2x^2$	$\lambda+\frac{1}{2}(a_1+a_8)\sigma_1=0$
Hex	(0,0,0,x,x)	$3x^2$	$\lambda+\frac{1}{6}(2a_1+a_3)\sigma_1=0$
Tri	$i(0,0,0,x,x)$	$3x^2$	$\lambda+\frac{1}{6}(2a_1+a_3)\sigma_1=0$
bcc	(x,x,x,x,x)	$6x^2$	$\lambda+\frac{1}{6}(a_1+a_3+a_8+a_{16})\sigma_1=0$
bccI	$i(x,x,x,x,x)$	$6x^2$	$\lambda+\frac{1}{6}(a_1+a_3+a_8-a_{16})\sigma_1=0$
123	(x,x,x,0,0)	$3x^2$	$\lambda+\frac{1}{6}(2a_1+a_3)\sigma_1=0$
A	(0,x,x,0,-x)	$4x^2$	$\lambda+\frac{1}{8}(2a_1+a_3+2a_8-a_{16})\sigma_1=0$
B	(0,x,x,0,x)	$4x^2$	$\lambda+\frac{1}{8}(2a_1+a_3+2a_8+a_{16})\sigma_1=0$

$$\lambda+a_{12}r+(a_1+a_3+a_8+a_{16})r^2=\frac{1}{4}\delta[\tilde{k}_i^2-1]^2+O(q^3,r^3) \tag{5.3}$$

$$-\delta\alpha_1[(\tilde{k}_1^2-1)(\tilde{k}_1\cdot\vec{k}')+(\tilde{k}_1\cdot\vec{k}')^2+\frac{1}{2}(\tilde{k}_1^2-1)k'^2]+O(k'^3;q^3,r^3).$$

with  $\tilde{k}_i^2$  the same for every  $i$ . The evolution equation for  $\alpha_1$  is

$$\begin{aligned} \dot{\alpha}_1 &= \frac{1}{2}a_{12}r(\alpha_2+\alpha_3+\alpha_5+\beta_6-2\alpha_1)+r^2[a_1(\alpha_1+\beta_1) \\ &+ \frac{1}{4}a_3(\alpha_2+\beta_2+\alpha_3+\beta_3+\alpha_5+\beta_5+\alpha_6+\beta_6)+a_8(\alpha_4 \\ &+ \beta_4)+\frac{1}{2}a_{16}(\alpha_2+\alpha_4+\alpha_5+\alpha_3+\beta_4+\beta_6-2\alpha_1)] \end{aligned}$$

Again, the result for  $\beta_1$  is similar, with  $\vec{k}' \rightarrow -\vec{k}'$  and  $\alpha \leftrightarrow \beta$ , and similarly for  $\alpha_2, \dots, \beta_6$ .

The linear problem can again be written in the form  $\dot{\xi} = (\mathbf{H}_0 + \mathbf{H}_1 + \mathbf{H}_2 + \mathbf{H}_3)\xi$  with  $\xi = (\alpha_1, \dots, \beta_6)$ , and is guaranteed to have real eigenvalues. To simplify the analysis we define  $\zeta = \frac{1}{2}a_{12}$ , assume the coefficients are in the ratio (5.2) and scale the amplitude  $r$  such that  $a_1 = -1$ . The lowest order matrix  $\mathbf{H}_0$  then has the orthogonal (but not normalized) eigenvectors  $(\phi_1, \dots, \phi_{12})$  given by the columns of

$$\Phi = \begin{pmatrix} 1 & 1 & 0 & 1 & 1 & 0 & 1 & 0 & 0 & 1 & 1 & 1 \\ -1 & -1 & 0 & -1 & -1 & 0 & 1 & 0 & 0 & 1 & 1 & 1 \\ 0 & 1 & 1 & -1 & 0 & 1 & 0 & 1 & 0 & -1 & 1 & 1 \\ 0 & -1 & -1 & 1 & 0 & -1 & 0 & 1 & 0 & -1 & 1 & 1 \\ 1 & 0 & 1 & 0 & -1 & -1 & 0 & 0 & 1 & 0 & -2 & 1 \\ -1 & 0 & -1 & 0 & 1 & 1 & 0 & 0 & 1 & 0 & -2 & 1 \\ 1 & -1 & 0 & -1 & 1 & 0 & -1 & 0 & 0 & 1 & 1 & 1 \\ -1 & 1 & 0 & 1 & -1 & 0 & -1 & 0 & 0 & 1 & 1 & 1 \\ 0 & 1 & -1 & -1 & 0 & -1 & 0 & -1 & 0 & -1 & 1 & 1 \\ 0 & -1 & 1 & 1 & 0 & 1 & 0 & -1 & 0 & -1 & 1 & 1 \\ -1 & 0 & 1 & 0 & 1 & -1 & 0 & 0 & -1 & 0 & -2 & 1 \\ 1 & 0 & -1 & 0 & -1 & 1 & 0 & 0 & -1 & 0 & -2 & 1 \end{pmatrix}$$

with corresponding eigenvalues

$$\{e_i\}_{i=1, \dots, 12} = r\{0, 0, 0, \underbrace{4(2r-\zeta)}_{\text{thrice}}, \underbrace{2(5r-\zeta)}_{\text{thrice}}, \underbrace{2(3r-2\zeta)}_{\text{twice}}, 2(-15r+\zeta)\}.$$

The first six eigenvectors are PM modes and the last six are AM modes, with the first three PM modes being translations in the  $x$ ,  $y$ , and  $z$  directions, respectively. In order for the bcc state to be stable with respect to perturbations on the bcc lattice, we demand that

$$\frac{1}{15} < \frac{r}{\zeta} < \frac{1}{5},$$

i.e., the bcc solution must have finite amplitude. This is a consequence of the fact that the bifurcation to the bcc state is transcritical, with the bcc state acquiring stability only at a secondary saddle-node bifurcation [7,18].

As before we define  $(A, B, C, D, E, F) \equiv (\hat{k}_1 \cdot \vec{k}'/k', \dots, \hat{k}_B \cdot \vec{k}'/k')$  and set

$$X = \hat{x} \cdot \vec{k}'/k', \quad Y = \hat{y} \cdot \vec{k}'/k', \quad Z = \hat{z} \cdot \vec{k}'/k',$$

giving us  $A = (X + Y)/\sqrt{2}$ , etc. In the following the PM

eigenvectors  $\langle \phi_4 |$ ,  $\langle \phi_5 |$ ,  $\langle \phi_6 |$  play no role and we delete them. The (non-normalized) first order perturbation matrix is therefore

$$\langle \phi_i | \mathbf{H}_1 | \phi_i \rangle_{i=7, \dots, 12}^{i=1,2,3} = 2\sqrt{2} \delta k' (\tilde{k}^2 - 1)$$

$$\times \begin{matrix} & i \rightarrow \\ l \downarrow & \begin{pmatrix} Y & X & 0 \\ 0 & Z & Y \\ Z & 0 & X \\ X & 0 & -Z \\ X & -2Y & Z \\ -2X & -2Y & -2Z \end{pmatrix} \end{matrix}.$$

The correctly normalized total perturbation matrix is

$$\begin{aligned} \mathbf{V}_{ij} + \langle \phi_i | \mathbf{H}_2 | \phi_j \rangle = -\delta^2 k'^2 (\tilde{k}^2 - 1)^2 & \left\{ \frac{1}{8r(5r - \zeta)} \begin{pmatrix} Y^2 + Z^2 & XY & XZ \\ XY & X^2 + Z^2 & YZ \\ XZ & YZ & X^2 + Y^2 \end{pmatrix} \right. \\ & - \frac{1}{24r(3r - 2\zeta)} \begin{pmatrix} 2X^2 & -XY & -XZ \\ -XY & 2Y^2 & -YZ \\ -XZ & -YZ & 2Z^2 \end{pmatrix} - \frac{1}{6r(-15r + \zeta)} \begin{pmatrix} X^2 & XY & XZ \\ XY & Y^2 & YZ \\ XZ & YZ & Z^2 \end{pmatrix} \left. \right\} \\ & - \frac{\delta}{4} k'^2 \begin{pmatrix} 2X^2 + Y^2 + Z^2 & 2XY & 2XZ \\ 2XY & X^2 + 2Y^2 + Z^2 & 2YZ \\ 2XZ & 2YZ & X^2 + Y^2 + 2Z^2 \end{pmatrix}. \end{aligned}$$

The substitutions  $\tilde{k} = \sqrt{1 + 2q}$ ,  $Z^2 = 1 - X^2 - Y^2$ , and

$$\zeta = \frac{\delta q^2 - \lambda + 15r^2}{2r}$$

[see Eq. (5.3)] allow us to write the eigenvalues of the above matrix as  $\delta k'^2$  times the solutions in  $t$  to

$$t^3 + \Delta t^2 + \Xi t + Y = 0,$$

where

$$\Delta = \frac{\delta N_\Delta}{(\lambda - \delta q^2 + 15r^2)(\lambda - \delta q^2 - 5r^2)(\lambda - \delta q^2 - 12r^2)},$$

$$\Xi = \frac{\delta^2 N_\Xi}{16(\lambda - \delta q^2 + 15r^2)(\lambda - \delta q^2 - 12r^2)^2(\lambda - \delta q^2 - 5r^2)^2},$$

$$Y = \frac{\delta^3 N_Y}{64(\lambda - \delta q^2 + 15r^2)(\lambda - \delta q^2 - 12r^2)^2(\lambda - \delta q^2 - 5r^2)^3},$$

and

$$\begin{aligned} N_\Delta = & \lambda^3 - 2\lambda^2 \delta q^2 + \lambda \delta^2 q^4 - 2\lambda^2 r^2 + 36\lambda \delta q^2 r^2 - 34\delta^2 q^4 r^2 \\ & - 195\lambda r^4 - 270\delta q^2 r^4 + 900r^6. \end{aligned}$$

The factors  $N_\Xi$  and  $N_Y$  are listed in Ref. [19]. All the expressions are functions of  $\delta q^2$ , so without loss of generality we set  $\delta = 1$  in what follows.

As in the fcc case it is helpful to look first at the coefficient  $\Delta$ . The requirement that the nontrivial eigenvalues  $e_i$  all be negative translates into the requirement

$$q^2 - 15r^2 < \lambda < q^2 + 5r^2,$$

providing a restriction on the denominator. This is the ‘‘smile’’ between the lower two parabolas in Fig. 5, drawn for  $r = \frac{1}{10}$ . The numerator  $N_\Delta$  vanishes along the other two curves shown in the figure. One resembles a parabola near

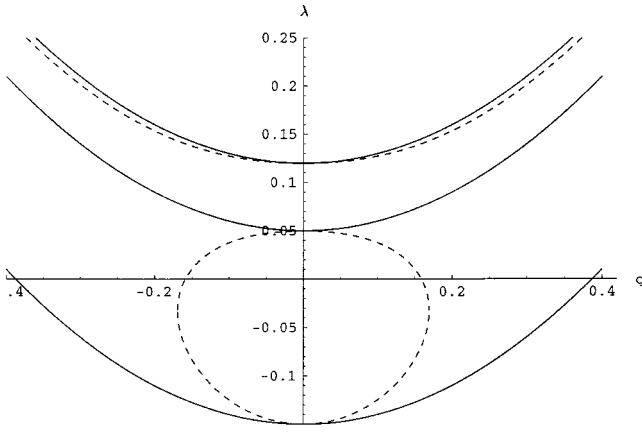


FIG. 5. The curves in the  $q$ - $\lambda$  plane across which  $\Delta$  for the bcc state changes sign when  $r = \frac{1}{10}$ . The denominator of  $\Delta$  vanishes along the solid parabolas and the numerator vanishes along the dashed curves. The undistorted ( $q=0$ ) bcc state is stable between the two lowest parabolas, and  $\Delta > 0$  in the “bubble” containing the origin.

$\lambda = q^2 + 12r^2$ , while the other is a small “bubble” entirely contained within the smile. Thus whatever complicated boundary we get for  $Y=0$ , we need only look at that portion within the bubble given by  $\Delta = 0$ .

We turn now to the coefficient  $Y$ . Figure 6 shows the

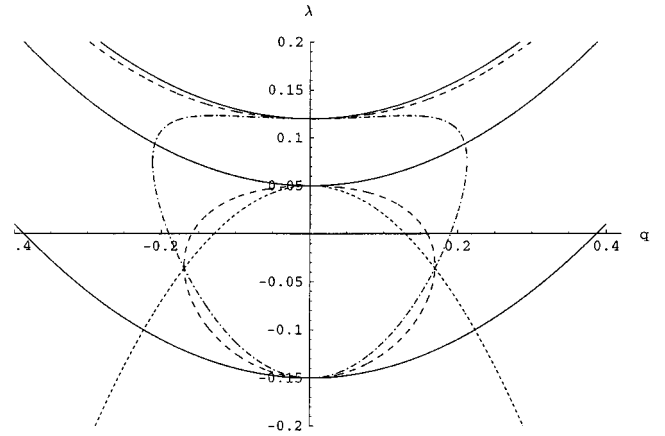


FIG. 6. The neutral stability curve for the bcc state together with the zeros of  $Y$  and  $\Delta$  when  $r = \frac{1}{10}$  for the case where  $\vec{k}'$  is parallel to the  $z$  axis, so that  $Z=1$  and the zeros of  $Y$  lie on the curve  $f_{z=1}=0$  and  $g_{z=1}=0$ . The solid and dashed curves are as in Fig. 5,  $f_{z=1}=0$  along the short dashed curve and  $g_{z=1}=0$  along the dot-dashed curve. The stability region is reduced to the eye-shaped region inside the bubble.

locus of points in the  $q$ - $\lambda$  plane for which  $Y$  vanishes for the particular direction cosines  $X=Y=0$  and  $Z=1$  along with the parabolas of marginal stability and the bubble  $N_\Delta=0$  from Fig. 5. This locus divides the smile into regions distinguished by the sign of  $Y$ . In fact,

$$Y(X=Y=0) = \frac{(\lambda + 3q^2 - 5r^2)^2(\lambda^2 - 4\lambda q^2 + 3q^4 + 3\lambda r^2 + 39q^2 r^2 - 180r^4)}{32(\lambda - q^2 - 12r^2)(\lambda - q^2 - 5r^2)^2(\lambda - q^2 + 15r^2)}.$$

Although  $Y(X=Y=0)$  does not change sign across the parabola  $\lambda + 3q^2 - 5r^2 = 0$  it turns out that the coefficient  $\Xi(X=Y=0)$  does. Thus  $\lambda + 3q^2 - 5r^2 = 0$  is a stability boundary, forming the top boundary of the eye-shaped region in Fig. 6 containing the origin. This region is defined by

$$f_{z=1} = \lambda + 3q^2 - 5r^2 < 0,$$

$$g_{z=1} = \lambda^2 - 4\lambda q^2 + 3q^4 + 3\lambda r^2 + 39q^2 r^2 - 180r^4 < 0$$

with  $g=0$  forming the bottom boundary. The resulting eye is entirely contained within the  $\Delta$  bubble, and remains so for all values of  $r$ . To show this we first show that the  $\Delta$  bubble  $N_\Delta=0$  intersects the parabola  $f_{z=1}=0$  at only two points other than  $q=0$ . Likewise  $g_{z=1}=N_\Delta=0$  has only two non-trivial solutions. Moreover, for each  $r$  there are two points in the  $q$ - $\lambda$  plane at which all three polynomials vanish. These results are conveniently proved using Gröbner bases; for details see Ref. [19]. Thus the eye is always entirely contained within the bubble with the corners of the eye exactly on the bubble, as shown in Fig. 6.

There are two other important cases:  $X=0$ ,  $Y=Z=1/\sqrt{2}$ , and  $X=Y=Z=1/\sqrt{3}$ . The former gives top and bottom boundaries

$$f_{X=0,Y=Z}=f_{Z=1}=0,$$

$$\begin{aligned} g_{X=0,Y=Z} &= 5\lambda^3 - 17\lambda^2 q^2 + 19\lambda q^4 - 7q^6 - 10\lambda^2 r^2 \\ &\quad + 232\lambda q^2 r^2 - 222q^4 r^2 - 975\lambda r^4 - 1155q^2 r^4 \\ &\quad + 4500r^6 = 0, \end{aligned}$$

while the latter has the boundaries

$$\begin{aligned} f_{X=Y=Z} &= \lambda^2 + \lambda q^2 - 2q^4 - 17\lambda r^2 - 12q^2 r^2 + 60r^4 = 0, \\ g_{X=Y=Z} &= \lambda^2 - 2\lambda q^2 + q^4 + 10\lambda r^2 + 30q^2 r^2 - 75r^4 = 0. \end{aligned}$$

The boundary  $f_{X=Y=Z}=0$  always lies above the boundary  $f_{z=1}=0$  and can be ignored. The three bubbles  $g=0$  for these three sets of direction cosines meet at the points  $(q^2, \lambda) = (\frac{21}{10}, -\frac{69}{10})r^2$ ; apart from these points and the point  $q=0$  there are no intersections between any two of them. Since these three bubbles cross transversely at their meeting

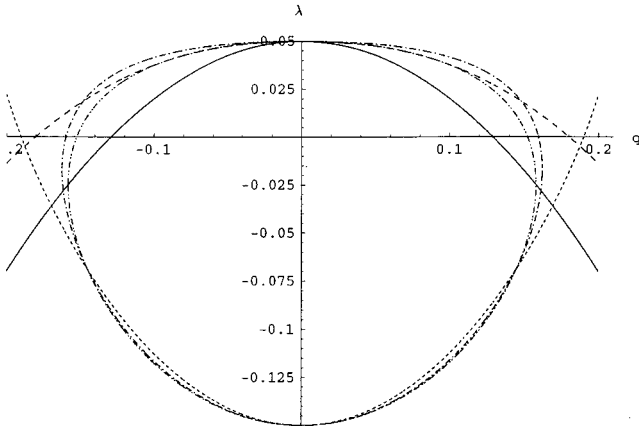


FIG. 7. The final region in the  $q$ - $\lambda$  plane (the Busse balloon) in which the bcc solution is stable to long-wavelength perturbations of arbitrary orientation, again for  $r = \frac{1}{10}$ . The region contains the origin and is bounded by the curves  $f_{z=1}=0$  (solid),  $g_{z=1}=0$  (short dashed), and  $g_{X=Y=Z}=0$  (dot-dot-dashed). Also shown are the curves where  $f_{X=Y=Z}=0$  (dashed) and  $g_{X=0,Y=Z=0}$  (dot-dashed).

point (their gradients point in different directions) the curve  $g_{X=0,Y=Z=0}$  can never form a part of the stability boundary. Thus the boundary of the eye is formed by  $g_{z=1}=0$  and  $g_{X=Y=Z}=0$  (see Fig. 7).

It remains to show that none of the other values of  $X$  and  $Y$  lie on the stability boundary. To construct the envelope of all such boundaries as  $(X, Y)$  ranges over the unit disk  $D^2$  we note that a point  $(q, \lambda)$  lies on this envelope when

$$(1) \quad \forall (X, Y) \in D^2: N_Y(\lambda, q, r, X, Y) \geq 0$$

and

$$(2) \quad \exists (X, Y) \in D^2: N_Y(\lambda, q, r, X, Y) = 0,$$

i.e.,  $(q, \lambda)$  on the envelope implies

$$\min_{(X, Y) \in D^2} N_Y(\lambda, q, r, X, Y) = 0.$$

Because of the permutation symmetry among  $X$ ,  $Y$ , and  $Z$ , points on the boundary of  $D^2$  are equivalent to points in the interior of the disk. Thus we wish to look for points  $(q, \lambda)$  such that there exist  $(X, Y) \in \text{int } D^2$  with the property

$$N_Y = \frac{\partial N_Y}{\partial X} = \frac{\partial N_Y}{\partial Y} = 0.$$

We find that

$$\frac{\partial N_Y}{\partial X} = 2X(1 - 2X^2 - Y^2)F(\lambda, q, r)G(\lambda, q, r, Y)$$

with

$$F(\lambda, q) = \lambda^2 + 4\lambda q^2 - 5q^4 - 17\lambda r^2 - 69q^2 r^2 + 60r^4,$$

$$\begin{aligned} G(\lambda, q, r, Y) = & 3\lambda^4 - 10\lambda^3 q^2 - 28\lambda^2 q^4 + 74\lambda q^6 - 39q^8 \\ & - 21\lambda^3 r^2 + 277\lambda^2 q^2 r^2 + 261\lambda q^4 r^2 - 517q^6 r^2 \\ & - 555\lambda^2 r^4 - 2860\lambda q^2 r^4 + 655q^4 r^4 + 5625\lambda r^6 \\ & + 8625q^2 r^6 - 13500r^8 - 5\lambda^4 Y^2 + 2\lambda^3 q^2 Y^2 \\ & + 96\lambda^2 q^4 Y^2 - 178\lambda q^6 Y^2 + 85q^8 Y^2 \\ & + 35\lambda^3 r^2 Y^2 - 319\lambda^2 q^2 r^2 Y^2 - 1339\lambda q^4 r^2 Y^2 \\ & + 1623q^6 r^2 Y^2 + 925\lambda^2 r^4 Y^2 + 7800\lambda q^2 r^4 Y^2 \\ & + 3315q^4 r^4 Y^2 - 9375\lambda r^6 Y^2 - 31275q^2 r^6 Y^2 \\ & + 22500r^8 Y^2. \end{aligned}$$

The expression for  $\partial N_Y / \partial Y$  is identical but with  $X, Y$  interchanged. We have already looked at the case where two of  $(X, Y, Z)$  vanish and at the case  $X=Y=Z$ . We now assume that neither of these is the case. If one of  $(X, Y, Z)$  vanishes we use our permutation symmetry and choose it to be  $Z$ . If two of  $(X, Y, Z)$  are equal, we choose  $Z$  to be the different one. Thus we can assume without loss of generality that  $X, Y \neq 0, Z$ . Now  $X \neq Z$  implies  $1 - 2X^2 - Y^2 \neq 0$  and similarly for  $1 - X^2 - 2Y^2$ . Furthermore,  $F(\lambda, q) = N_Y = 0$  is solved by the points  $(q^2, \lambda) = (\frac{21}{10}, -\frac{69}{10})r^2$  already identified, independently of the direction cosines. This is not surprising, as at this point  $Y$  vanishes for all  $(X, Y)$ . If  $X^2 \neq Y^2$  and  $qr \neq 0$ , the remaining factors  $G(\lambda, q, r, Y)$ ,  $G(\lambda, q, r, X)$  vanish together with  $Y$  at  $q^2 = -\lambda = 5r^2/2$ , i.e., another pair of isolated points on a boundary we already have, namely,  $f_{z=1} = 0$ . We therefore assume that  $X=Y$ , obtaining the two possibilities

$$\begin{aligned} g_{\text{general},1} \equiv & \lambda^3 - 3\lambda^2 q^2 - 5\lambda q^4 + 7q^6 - 2\lambda^2 r^2 + 80\lambda q^2 r^2 \\ & + 26q^4 r^2 - 195\lambda r^4 - 465q^2 r^4 + 900r^6 = 0, \end{aligned}$$

$$\begin{aligned} g_{\text{general},2} \equiv & \lambda^3 - 4\lambda^2 q^2 + 5\lambda q^4 - 2q^6 - 2\lambda^2 r^2 + 52\lambda q^2 r^2 \\ & - 50q^4 r^2 - 195\lambda r^4 - 300q^2 r^4 + 900r^6 = 0. \end{aligned}$$

The bubble  $g_{\text{general},1} = 0$  intersects  $f_{z=1} = 0$  and  $g_{X=Y=Z} = 0$  at the same point. The additional requirement that the extremum lies in the unit disk, so that  $X^2 \leq \frac{1}{2}$ , is only satisfied for that portion of the bubble above its intersection with  $g_{X=Y} = 0$ . Thus the physically meaningful portion of the boundary  $g_{\text{general},1} = 0$  does not intersect the region of stability we have already found. A similar result holds for  $g_{\text{general},2}$ . These results are again conveniently proved using Gröbner bases.

In summary, the bcc state is stable with respect to long-wavelength perturbations in the small region of the  $q$ - $\lambda$  plane defined by

$$f_{Z=1} < 0, \quad g_{Z=1} < 0, \quad g_{X=Y=Z} < 0,$$

shown in Fig. 7. At the boundary  $f_{Z=1} = 0$  there are two null eigenvectors  $(1,0,0)$  and  $(0,1,0)$ . Thus we have a zigzag instability with the wave vector along a coordinate axis but no polarization preference. At  $g_{Z=1} = 0$  there is the single null eigenvector  $(0,0,1)$ , so this is an Eckhaus instability along a coordinate axis. At  $g_{X=Y=Z} = 0$  the null eigenvector is  $(1,1,1)$ , so there is an Eckhaus instability along the body diagonal of the cube.

### C. The solution bccI

We now examine the bccI solution  $z_1 = \dots = z_6 = ir$  in the same regime (5.2) as the bcc solution in the previous section. The distorted equilibrium is given by

$$\lambda + (a_1 + a_3 + a_8 - a_{16})r^2 = \frac{1}{4}\delta(\tilde{k}^2 - 1)^2 + O(q^3, r^3)$$

and its perturbation, defined by

$$\{e_i\}_{i=1, \dots, 12} = r\{0, 0, 0, -14r, -2r, -2r, \underbrace{-7r - \sqrt{r^2 + 8\zeta^2}}_{\text{thrice}}, \underbrace{-7r + \sqrt{r^2 + 8\zeta^2}}_{\text{thrice}}\}.$$

Since the last eigenvalue is positive when  $r$  is small, the undistorted ( $q=0$ ) bccI solution is unstable at the onset and only acquires stability at finite amplitude.

The first six eigenvalues belong to the orthogonal eigenvectors

$$(\phi_1, \dots, \phi_6) = \begin{pmatrix} 1 & 1 & 0 & -1 & -1 & 1 \\ -1 & -1 & 0 & -1 & -1 & 1 \\ 0 & 1 & 1 & 0 & 2 & 1 \\ 0 & -1 & -1 & 0 & 2 & 1 \\ 1 & 0 & 1 & 1 & -1 & 1 \\ -1 & 0 & -1 & 1 & -1 & 1 \\ 1 & -1 & 0 & -1 & -1 & 1 \\ -1 & 1 & 0 & -1 & -1 & 1 \\ 0 & 1 & -1 & 0 & 2 & 1 \\ 0 & -1 & 1 & 0 & 2 & 1 \\ -1 & 0 & 1 & 1 & -1 & 1 \\ 1 & 0 & -1 & 1 & -1 & 1 \end{pmatrix}.$$

The first three of these are PM modes corresponding to translations in the  $x$ ,  $y$ , and  $z$  directions, while the last three are

$$z_j = ie^{i\tilde{q}_j \cdot \tilde{x}}(r + \alpha_j e^{i\tilde{k}' \cdot \tilde{x}} + \bar{\beta}_j e^{-i\tilde{k}' \cdot \tilde{x}}),$$

evolves according to

$$\begin{aligned} \dot{\alpha}_1 = & ir\zeta(-\alpha_2 + \alpha_3 + \alpha_5 - \beta_6) + a_1 r^2(\alpha_1 + \beta_1) \\ & + \frac{1}{2}a_3 r^2(\alpha_2 + \beta_2 + \alpha_3 + \beta_3 + \alpha_5 + \beta_5 + \alpha_6 + \beta_6) \\ & + a_8 r^2(\alpha_4 + \beta_4) - \frac{1}{2}a_{16} r^2 \\ & \times (\alpha_2 + \alpha_4 + \alpha_5 + \alpha_3 + \beta_4 + \beta_6 - 2\alpha_1) \\ & - \delta\alpha_1[(\tilde{k}^2 - 1)(\tilde{k} \cdot \tilde{k}') + (\tilde{k} \cdot \tilde{k}')^2 + \frac{1}{2}(\tilde{k}^2 - 1)k'^2]. \end{aligned}$$

The equation for  $\dot{\beta}_1$  is obtained by interchanging  $\alpha_i$  and  $\beta_i$  and changing the sign of  $\zeta$ , etc. As in the bcc case we assume that the coefficients are in the ratio (5.2) with  $a_1 = -1$ . The lowest order matrix  $\mathbf{H}_0$  is now complex, but is still Hermitian, and so still has only real eigenvalues,

AM modes. The remaining six eigenvectors are superpositions of AM and PM modes. Using the orthogonal vectors

$$(\psi_7, \dots, \psi_{12}) = \begin{pmatrix} 0 & 0 & -6 & 0 & 2 & 1 \\ 0 & 0 & -2 & 2 & 0 & -3 \\ 1 & -1 & 1 & -1 & 0 & -3 \\ 3 & 0 & 3 & 0 & 2 & 1 \\ 3 & 0 & 1 & 2 & -1 & 1 \\ 1 & -1 & -5 & -1 & -1 & 1 \\ -2 & -1 & 4 & -1 & -1 & 1 \\ 2 & 1 & 4 & -1 & -1 & 1 \\ -3 & 0 & 1 & 2 & -1 & 1 \\ -1 & 1 & -5 & -1 & -1 & 1 \\ -3 & 0 & 3 & 0 & 2 & 1 \\ -1 & 1 & 1 & -1 & 0 & -3 \end{pmatrix},$$

we normalize the basis  $(\phi_1, \dots, \phi_6, \psi_7, \dots, \psi_{12})$  and block diagonalize  $\mathbf{H}_0$  in this basis to get



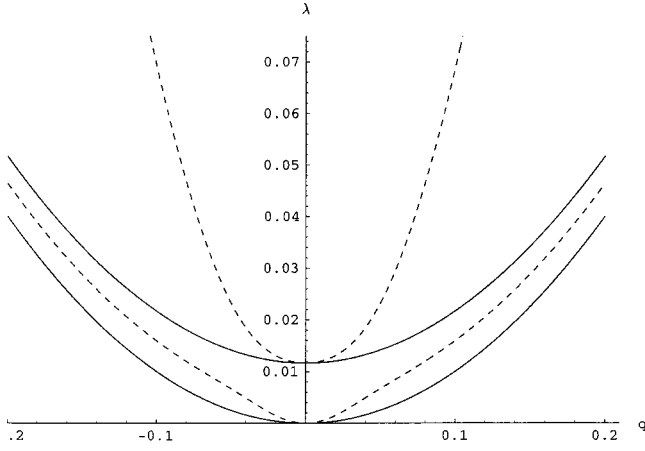


FIG. 8. The equivalent of Fig. 5 for the bccI solution. There are two parabolic neutral stability curves (solid) and a locus of points for which  $\Delta=0$  (dashed). For this and the following figure we have chosen  $\zeta = \frac{1}{10}$ .

where we have chosen to eliminate  $r$  instead of  $\zeta$ . Once again the expressions for  $N_{\Xi}$  and  $N_Y$  are too long to list [19].

We set  $\delta=1$  and examine the roots of this equation subject to the requirement that the bccI state is stable with respect to perturbations on the lattice, i.e., that the nontrivial eigenvalues  $e_i$  be negative. This occurs in the region

$$\lambda > q^2 + \frac{7}{6}\zeta^2.$$

This is the region above the upper parabola in Fig. 8, drawn for  $\zeta = \frac{1}{10}$ . The coefficient  $\Delta$  is positive above this curve and negative below it, i.e., the region of long-wavelength stability must be entirely above the upper parabola in Fig. 8. We next examine the coefficient  $Y$ . For the particular direction cosines  $X=Y=0$  and  $Z=1$ ,

$$Y(X=Y=0) = \frac{(\lambda - 7q^2)(6\lambda - 34q^2 - 7\zeta^2)^2}{32(\lambda - q^2)(6\lambda - 6q^2 - 7\zeta^2)^2},$$

which vanishes when

$$f_{Z=1} \equiv \lambda - 7q^2 = 0,$$

$$g_{Z=1} \equiv 6\lambda - 34q^2 - 7\zeta^2 = 0.$$

As in the bcc case,  $\Xi(X=Y=0)$  changes sign across  $g_{Z=1}=0$ , i.e.,  $g_{Z=1}=0$  is a stability boundary. Moreover, these two curves always intersect on the curve  $N_{\Delta}=0$ , so that the region of stability must be contained within the region defined by  $f_{Z=1}>0$  and  $g_{Z=1}>0$ . The other two special directions are  $X=0$ ,  $Y=Z=1/\sqrt{2}$ , and  $X=Y=Z=1/\sqrt{3}$ . In the former case  $Y$  vanishes for  $g_{Z=1}=0$  and

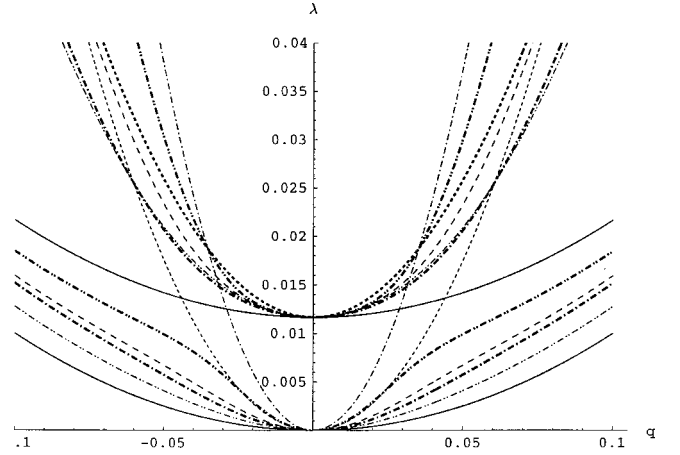


FIG. 9. The region of stability in the  $q$ - $\lambda$  plane for which the bccI solution is stable to long-wavelength perturbations. This is the upper central region lying above the curves  $f_{X=0,Y=Z}=0$ ,  $g_{Z=1}=0$ . The solid and dashed curves are as in Fig. 8. The curves  $f_{Z=1}=0$ ,  $f_{X=0,Y=Z}=0$ , and  $f_{X=Y=Z}=0$  are drawn short dashed, dot-dashed, and dot-dot-dashed, respectively. The curves for  $g_{Z=1}=0$ , etc. are drawn the same way except in bold.

$$f_{X=0,Y=Z} \equiv \lambda - 15q^2 = 0,$$

$$g_{X=0,Y=Z} \equiv 30\lambda^2 - 176\lambda q^2 + 146q^4 - 35\lambda\zeta^2 + 105q^2\zeta^2 = 0,$$

while in the latter case  $Y$  vanishes for

$$f_{X=Y=Z} \equiv 6\lambda^2 - 32\lambda q^2 + 26q^4 - 7\lambda\zeta^2 + 14q^2\zeta^2 = 0,$$

$$g_{X=Y=Z} \equiv 6\lambda^2 - 68\lambda q^2 + 62q^4 - 7\lambda\zeta^2 + 56q^2\zeta^2 = 0.$$

In the latter case  $Y$  contains a factor  $g_{X=Y=Z}^2$ , but  $\Xi$  changes sign across this curve indicating that  $g_{X=Y=Z}=0$  is a stability boundary. The same techniques used for the bcc solutions can now be used to determine the stability boundary for the bccI solution. We find that the curves  $f_{X=0,Y=Z}=0$ ,  $g_{Z=1}=0$ , and  $g_{X=Y=Z}=0$  meet at the points  $(q^2, \lambda) = (\frac{1}{8}, \frac{15}{8})\zeta^2$ , while the curves  $f_{Z=1}=0$ ,  $f_{X=Y=Z}=0$ , and  $g_{X=0,Y=Z}=0$  meet at  $(q^2, \lambda) = (\frac{35}{96}, \frac{245}{96})\zeta^2$ . The region of stability is therefore delineated by the boundaries  $g_{Z=1}=0$  and  $f_{X=0,Y=Z}=0$  as shown in Fig. 9. This stability picture is unchanged when general orientations of  $\vec{k}'$  are included. The same analysis as for the bcc pattern leads to a pair of functions  $F(\lambda, q, \zeta)$  and  $G(\lambda, q, \zeta, X)$  whose explicit forms we omit. The possibility  $F(\lambda, q, \zeta)=0$  leads to the intersection points already found, while the possibilities  $G(\lambda, q, \zeta, X)=G(\lambda, q, \zeta, Y)=0$  and  $X^2 \neq Y^2$  lead to the first of the above intersection points. Finally, the possibility  $G(\lambda, q, \zeta, X)=G(\lambda, q, \zeta, Y)=0$  and  $X=Y$  leads to another set of boundaries, which, just as for the bcc solution, do not enter the stability region already identified.

The net result is that the stability of the bccI state is delimited by two boundaries in the  $q$ - $\lambda$  plane. The lower boundary is given by  $g_{z=1}=0$  and holds for  $q^2 < \zeta^2/8$  or  $\lambda < 15\zeta^2/8$ . Along this boundary, the null eigenvectors of  $\mathbf{V}_{ij} + \langle \phi_i | \mathbf{H}_2 | \phi_j \rangle$  are (1,0,0) and (0,1,0) corresponding to a zigzag instability along this boundary with wave vector along a coordinate axis and no polarization preference. The upper boundary is  $f_{X=0,Y=Z}=0$ , and holds for  $q^2 > \zeta^2/8$  or  $\lambda > 15\zeta^2/8$  (see Fig. 9). Along this boundary, the null eigenvector is (0,1,-1). This is another zigzag instability, this

time with wave vector along a diagonal in a coordinate plane and polarization in the same coordinate plane.

### C. The hex prisms

The hex prisms take the form  $r_1=r_2=r_3=0$  and  $r_4=r_5=r_6=r$ . The stability matrix  $\mathbf{H}_0$  has non-normalized but orthogonal eigenvectors

$$\Phi = \begin{pmatrix} 0 & 0 & 0 & 0 & 0 & 0 & 0 & -1 & 0 & -1 & 0 & 1 \\ 0 & 0 & 0 & 0 & 0 & 0 & -1 & 0 & -1 & 0 & 1 & 0 \\ 0 & 0 & 0 & 0 & 0 & 0 & 0 & 0 & 0 & 2 & 0 & 1 \\ 0 & 0 & 0 & 0 & 0 & 0 & 0 & 0 & 2 & 0 & 1 & 0 \\ 0 & 0 & 0 & 0 & 0 & 0 & 0 & 1 & 0 & -1 & 0 & 1 \\ 0 & 0 & 0 & 0 & 0 & 0 & 1 & 0 & -1 & 0 & 1 & 0 \\ 1 & 1 & 1 & 1 & 1 & 1 & 0 & 0 & 0 & 0 & 0 & 0 \\ -1 & -1 & -1 & 1 & 1 & 1 & 0 & 0 & 0 & 0 & 0 & 0 \\ 0 & -2 & 1 & 0 & -2 & 1 & 0 & 0 & 0 & 0 & 0 & 0 \\ 0 & 2 & -1 & 0 & -2 & 1 & 0 & 0 & 0 & 0 & 0 & 0 \\ -1 & 1 & 1 & -1 & 1 & 1 & 0 & 0 & 0 & 0 & 0 & 0 \\ 1 & -1 & -1 & -1 & 1 & 1 & 0 & 0 & 0 & 0 & 0 & 0 \end{pmatrix},$$

with eigenvalues

$$\{e_{ij}\}_{i=1,\dots,12} = r \{0, 0, -3\underbrace{\zeta, (2a_1 - \frac{1}{2}a_3)r - 2\underbrace{\zeta, (2a_1 + a_3)r + \zeta, (-a_1 - \frac{1}{2}a_{16} + a_8)r - 2\underbrace{\zeta, (-a_1 + a_{16} + a_8)r + \zeta}_{\text{twice}}}_{\text{twice}}}_{\text{four times}}\},$$

respectively. The null eigenvector  $|\phi_1\rangle$  represents a shift of the maxima in the direction  $(2\hat{x} - \hat{y} - \hat{z})/\sqrt{6}$ , while  $|\phi_2\rangle$  represents a shift in the direction  $(\hat{z} - \hat{y})/\sqrt{2}$ . Consequently the distorted equilibrium

$$\lambda + \zeta r + (a_1 + \frac{1}{2}a_3)r^2 = \frac{1}{4}\delta(\tilde{k}_4^2 - 1)^2 + O(q^3, r^3) \quad (5.4)$$

can have at most two unstable modes.

The properly normalized first order perturbation theory for  $\mathbf{H}_2$  yields

$$\langle \phi_i | \mathbf{H}_2 | \phi_j \rangle |_{i,j=1,2} = -\frac{1}{2}\delta k'^2 \begin{pmatrix} D^2 + F^2 & \frac{D^2 - F^2}{\sqrt{3}} \\ \frac{D^2 - F^2}{\sqrt{3}} & \frac{D^2 + 4E^2 + F^2}{3} \end{pmatrix}.$$

For second order perturbation theory for  $\mathbf{H}_1$  we first calculate the properly normalized

$$\langle \phi_l | \mathbf{H}_1 | \phi_i \rangle \Big|_{i=3, \dots, 12}^{i=1,2} = -\frac{1}{2} \delta k' (\tilde{k}^2 - 1) \begin{pmatrix} l \downarrow & i \rightarrow \\ 0 & 0 \\ D+F & \frac{D-F}{\sqrt{3}} \\ \frac{D-F}{\sqrt{3}} & \frac{D+4E+F}{3} \\ \sqrt{\frac{2}{3}}(D-F) & \frac{\sqrt{2}(D-2E+F)}{3} \\ 0 & 0 \\ 0 & 0 \\ 0 & 0 \\ 0 & 0 \\ 0 & 0 \\ 0 & 0 \end{pmatrix}.$$

The second order matrix is therefore

$$\mathbf{V}_{ij} = -\frac{\delta^2 k'^2 (\tilde{k}^2 - 1)^2}{(2a_1 - \frac{1}{2}a_3)r^2 - 2\zeta r} \begin{pmatrix} \frac{D^2 + DF + F^2}{3} & \frac{(D-F)(D+E+F)}{3\sqrt{3}} \\ \frac{(D-F)(D+E+F)}{3\sqrt{3}} & \frac{D^2 + 2DE + 4E^2 - DF + 2EF + F^2}{9} \end{pmatrix} \\ - \frac{\delta^2 k'^2 (\tilde{k}^2 - 1)^2}{(2a_1 + a_3)r^2 + \zeta r} \begin{pmatrix} \frac{(D-F)^2}{6} & \frac{(D-F)(D-2E+F)}{6\sqrt{3}} \\ \frac{(D-F)(D-2E+F)}{6\sqrt{3}} & \frac{(D-2E+F)^2}{18} \end{pmatrix}.$$

As before, we write  $\tilde{k} = \sqrt{1+2q}$  and  $A = (X+Y)/\sqrt{2}$ , etc., and use the equilibrium condition (5.4) in the form

$$\zeta = \frac{\delta q^2 - \lambda - (a_1 + \frac{1}{2}a_3)r^2}{r}$$

to obtain an equation for the eigenvalues of the perturbation matrix  $\mathbf{V}_{ij} + \langle \phi_i | \mathbf{H}_2 | \phi_j \rangle$  describing the long-wavelength properties of distorted hex prisms. These are  $\delta k'^2$  times the solutions in  $t$  to the *quadratic*

$$t^2 + \Delta t + \Xi = 0.$$

We evaluate the coefficients at  $(a_1, a_3, a_8, a_{16}) \approx -(1, 8, 2, 4)$ , obtaining

$$\Delta = \frac{2(X^2 - XY + Y^2 - XZ - YZ + Z^2)N_\Delta}{3(\lambda - \delta q^2 - 4r^2)(\lambda - \delta q^2 + 5r^2)},$$

$$\Xi = \frac{(\lambda + \delta q^2 - 4r^2)(X^2 - XY + Y^2 - XZ - YZ + Z^2)^2 N_\Xi}{12(\lambda - \delta q^2 - 4r^2)^2 (\lambda - \delta q^2 + 5r^2)}$$

and

$$N_\Delta = \lambda^2 - 3\lambda \delta q^2 + 2\delta^2 q^4 + \lambda r^2 + 12\delta q^2 r^2 - 20r^4$$

and

$$N_\Xi = \lambda^2 - 4\lambda \delta q^2 + 3\delta^2 q^4 + \lambda r^2 + 13\delta q^2 r^2 - 20r^4.$$

The denominators vanish along two parabolas and the hex prisms are stable only within the ‘‘smile’’ between them. Moreover,  $\Delta > 0$  inside the bubble given by  $N_\Delta = 0$ , while  $\Xi$  is positive below the parabola

$$f_\Xi = \lambda + \delta q^2 - 4r^2 = 0$$

and inside the curve  $N_\Xi = 0$ . Just as for the bcc solution, we can show that these three curves always meet at the point  $(q^2, \lambda) = (\frac{3}{2}, \frac{5}{2})r^2$ , and that the hex prisms can only be stable

for  $f_{\Xi} < 0$  and  $N_{\Xi} < 0$ . This is the region depicted in Fig. 10. Along the boundary  $f_{\Xi} = 0$ , the null eigenvector is  $-\sqrt{3}(Z - Y)|\phi_1\rangle + (2X - Y - Z)|\phi_2\rangle$ . Since  $|\phi_1\rangle$  is a shift by an amount  $(2\hat{x} - \hat{y} - \hat{z})/\sqrt{6}$ , while  $|\phi_2\rangle$  is a shift by an amount  $(\hat{z} - \hat{y})/\sqrt{2}$ , we recognize this as a zigzag instability with no preferred direction for  $\vec{k}'$ . At the boundary  $N_{\Xi} = 0$ , the null eigenvector is  $(2X - Y - Z)|\phi_1\rangle + \sqrt{3}(Z - Y)|\phi_2\rangle$ , indicating a skew-varicose instability.

In the special case  $X = Y = Z = 1/\sqrt{3}$  both  $\Delta$  and  $\Xi$  vanish. In this case we must go to higher order in  $k'$ . For this direction of  $\vec{k}'$ , both  $\langle \phi_i | \mathbf{H}_2 | \phi_j \rangle$  and  $\langle \phi_i | \mathbf{H}_1 | \phi_i \rangle$  vanish identically. The only term at the relevant order is

$$\langle \phi_i | \mathbf{H}_3 | \phi_j \rangle = -\frac{\delta}{2}(\tilde{k}^2 - 1)k'^2 \mathbf{1} = -\delta q k'^2 \mathbf{1}.$$

Thus if  $q < 0$  the system is unstable to both  $|\phi_1\rangle$  and  $|\phi_2\rangle$ , and this is a zigzag instability, with  $\vec{k}'$  pointed along the axis of the hexagonal prisms and no preference for polarization.

Once again, the long-wavelength stability properties of the lamellas are the same as those on the sc lattice. Moreover, with  $(a_1, a_3, a_8, a_{16}) \approx -(1, 8, 2, 4)$  the remaining primary branch, square prisms, is unstable even when  $q = 0$ . Consequently, we do not consider this state further.

## VI. TURING INSTABILITY

In the foregoing discussion we have taken an entirely model-independent approach so that the results are applicable to any three-dimensional pattern-forming system. In this section we indicate briefly the application of the preceding results to two two-species reaction-diffusion systems commonly used as models for the Turing instability. The first of these is the Brusselator model [20],

$$\begin{aligned} \dot{X} &= -(B+1)X + X^2Y + A + D_X \nabla^2 X, \\ \dot{Y} &= BX - X^2Y + D_Y \nabla^2 Y. \end{aligned} \quad (6.1)$$

Here  $X$  and  $Y$  are the chemical concentrations of an activator and an inhibitor, respectively,  $D_X$  and  $D_Y$  are their diffusivities ( $D_X < D_Y$ ), and  $A$  and  $B$  are parameters that are held fixed. Traditionally,  $B$  is chosen as the bifurcation parameter. As  $B$  increases through a critical value  $B_T$  three-dimensional structures may form. Indeed such structures were found in numerical simulations of the model [21,22].

Although the Brusselator has been much studied as a model system exhibiting a Turing instability, it is not a model for any specific chemical system *per se*. In contrast the second system, the Lengyel-Epstein model [23], models the chlorite-iodide-malonic acid reaction in which the Turing instability was first experimentally established [2]. More precisely, the Lengyel-Epstein (LE) model describes the closely related chlorine-dioxide-iodine-malonic acid reaction, which also exhibits the Turing instability. Like the Brusselator the Lengyel-Epstein model is a two-species model with one equation for an activator ( $\Gamma^-$ ) and another for an inhibitor ( $\text{ClO}_2^-$ ). In dimensionless variables the model takes the form

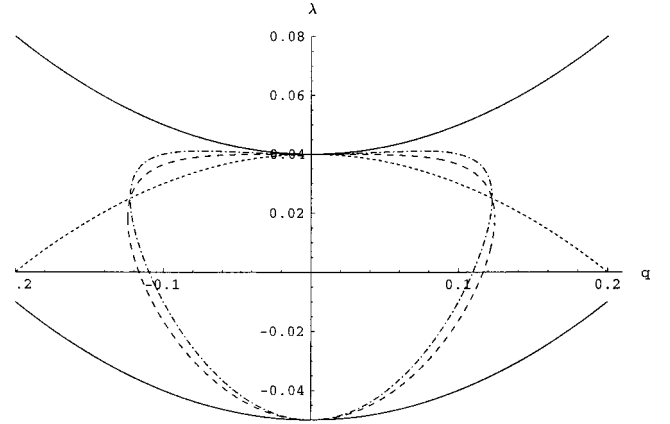


FIG. 10. The region in the  $q$ - $\lambda$  plane for which the hexagonal prism solution is stable to long-wavelength perturbations for  $r = \frac{1}{10}$ . This is the right half of the innermost region, bounded by the curves  $f_{\Xi} = 0$  (short dashed),  $N_{\Xi} = 0$  (dot-dashed), and  $q = 0$ . Also shown are the parabolas (solid) along which the denominator of  $\Delta$  vanishes and the curve (dashed) along which the numerator of  $\Delta$  vanishes.

$$\dot{X} = a - X - \frac{4XY}{1 + X^2} + \nabla^2 X, \quad (6.2)$$

$$\dot{Y} = \delta_{\text{LE}} \left[ b \left( X - \frac{XY}{1 + X^2} \right) + c \nabla^2 Y \right],$$

where  $X$  and  $Y$  again represent the activator and inhibitor concentrations,  $c$  is the ratio of their diffusivities, and  $a$  and  $b$  are fixed parameters. In aqueous solution  $c$  is generally close to 1 and consequently the conditions for the Turing instability are not satisfied. However, with starch present the iodide mobility is dramatically reduced (because of the binding of  $\text{I}^-$  to the starch) and the effective diffusivity ratio becomes larger by the factor  $\delta_{\text{LE}} > 1$ . Thus the starch plays a vital though passive role in the appearance of the instability [24]. Both models require four parameters for their complete specification. We think of two of these,  $A$  and  $B$  (resp.,  $a, b$ ), as representing concentrations of input chemicals, while the remaining two specify the diffusion rates of the activator and inhibitor. Moreover, in each model, the nonlinear term in the activator equation is of the same form as that in the inhibitor equation. This result of the law of mass action has important consequences for the properties of these models.

The nonlinear coefficients for these two models on the sc, fcc, and bcc lattices are calculated elsewhere [18] on the assumption that the wave number of the pattern is the Turing wave number  $k_T$  identified below. On the bcc lattice the coefficients are restricted by the relation (5.2) in order that stable patterns exist at small amplitude, i.e., in the range of validity of the amplitude equations. In the absence of degeneracies among these coefficients the nonlinear terms are unaffected by small departures of the wave number from  $k_T$ , i.e., by small distortions of the pattern. It remains therefore to calculate the neutral curve for the Turing instability as a

function of  $k - k_T$  and thereby identify the remaining coefficient  $\delta$  [see Eq. (3.1)] in the theory.

The Brusselator model has a uniform equilibrium at  $(X, Y) = (A, B/A)$ . Perturbations of this state with spatial dependence  $e^{i\vec{k}\cdot\vec{x}}$ , where  $\vec{k} \equiv \vec{k}_T + \vec{q}$ , are marginally stable when the determinant of the stability matrix

$$\begin{pmatrix} -D_X \tilde{k}^2 + B - 1 & A^2 \\ -B & -D_Y \tilde{k}^2 - A^2 \end{pmatrix}$$

vanishes, yielding the neutral stability curve

$$B = D_X \tilde{k}^2 + \left( 1 + A^2 \frac{D_X}{D_Y} \right) + \frac{A^2}{D_Y \tilde{k}^2}.$$

The Turing instability therefore sets in at the minimum of this curve, which is at

$$B = B_T \equiv [1 + A \sqrt{D_X/D_Y}]^2, \quad k^2 = k_T^2 \equiv \frac{A}{\sqrt{D_X D_Y}}.$$

We rescale the spatial coordinates so that  $k_T = 1$  (hence  $D_Y = A^2/D_X$ ) and henceforth write the critical wave vectors as  $\hat{k}$ . The procedure of Sec. II applied to  $B - B_T$  now yields an equation of the form (2.1) with

$$\lambda = \begin{cases} \frac{A^2}{(A^2 - R^2)(R + 1)} (B - B_T) & \text{for the Brusselator} \\ -\frac{25a \delta_{LE}}{(c \delta_{LE} - 1)R(25 + a^2)^{3/2}} (b - b_T) & \text{for the LE model,} \end{cases}$$

$$\delta = \begin{cases} \frac{4A^2}{(A^2 - R^2)(R + 1)} & \text{for the Brusselator} \\ \frac{5c \delta_{LE}}{\sqrt{10a}(c \delta_{LE} - 1)R} & \text{for the LE model.} \end{cases}$$

For pattern formation from a stable uniform state we must have  $\delta > 0$ . In these expressions  $R = A \sqrt{D_X/D_Y}$ , and  $-5 + \sqrt{40a^2/(25 + a^2)}$ , respectively. Calculations of the coefficient of the quadratic equivariant on the bcc lattice shows that this coefficient vanishes when  $R = 1$  (Brusselator) and  $\sqrt{21} - 4$  (Lengyel-Epstein) [18].

## VII. DISCUSSION

In this paper we have examined the stability of various steady three-dimensional patterns with cubic symmetry with respect to long-wavelength perturbations. The study was motivated by the Turing instability in three dimensions and focused on instabilities that restrict the wave number of the pattern. The analysis relies heavily on an existing analysis of three-dimensional patterns on the simple, face-centered- and body-centered-cubic lattices [7] and the application of this theory to reaction-diffusion systems that are used to model

the Turing instability [18]. To perform it we considered ‘‘isotropic’’ distortions of the patterns, i.e., distortions that change the length of all the wave vectors by the *same* amount. Anisotropic distortions such as those leading to rhombs in two dimensions [17] were not considered. The analysis identified various skew-varicose, zigzag, and Eckhaus instabilities that set in when the distortion becomes too large. We expect that the resulting instabilities will alter the wave number of the pattern in such a way that the local wave number everywhere falls in the stable region we identify. By analogy with the processes that accomplish this task in two dimensions we anticipate the existence of various gliding and climbing dislocations [1] by which the three-dimensional patterns adjust their wavelength. We have not, however, studied these processes in detail. In fact it is a relatively simple matter, although beyond the scope of the present paper, to derive phase equations describing the relaxation of the spatial phase of the pattern, cf. Refs. [25] and [11]. For three-dimensional patterns this process will be described by three phase equations coupled via nonlinear terms. Undoubtedly such equations describe a wealth of complex dynamics.

We found that patterns stable at the band center (i.e., with  $q = 0$ ) remain stable with respect to long-wavelength perturbations in some region of the  $q$ - $\lambda$  parameter plane. Here  $q$  specifies the change in the wave number away from  $k_T$  while the bifurcation parameter  $\lambda$  indicates the amplitude of the pattern. The resulting region of stability, referred to as the Busse balloon by analogy with the analogous problem in two dimensions, may be either open or closed at the ‘‘top,’’ i.e., at large  $\lambda$ . The latter is the case for the bcc and hexagonal prism solutions. Both these branches arise in a transcritical primary bifurcation, and gain and lose stability through secondary bifurcations [7]: for the coefficients calculated from the two-species reaction-diffusion equations, the bcc solutions gain stability at a saddle-node bifurcation and lose it by shedding a branch called  $123'$  while the hexagonal prism branch gains stability by shedding  $123'$  and loses it by shedding a branch of rhombic prisms. Consequently the Busse balloon must be closed at the band center, i.e., at  $q = 0$ . Although there is, in principle, no reason why the stability region should be closed for other values of  $q$  we find that this is in fact so. It should be noted, however, that with sufficiently *large* but even  $O(\square^3, \mathbf{z}^3)$  terms included in Eq. (5.1), the stability regions may become open [26]. Moreover, on the hexagonal lattice in two dimensions with the midplane symmetry  $\mathbf{z} \rightarrow -\mathbf{z}$  it is possible for hexagons  $H^\pm$  to be stable at large  $\lambda$  [27]; stable solutions of this type were recently computed for the Bénard problem [28] and exist for  $q$  sufficiently different from 0. In this case the Busse balloon for  $H^\pm$  remains open, and by continuity we expect this to be so for  $a_{12} \ll 1$  as well. We remark that standing waves in the parametrically forced Hopf bifurcation also have a closed Busse balloon [29]. This example is interesting because the standing waves do not lose stability with increasing  $\lambda$  in the absence of sideband perturbations. In cases in which the stability region for a solution is open, other techniques must be employed to find (finite wavelength) instabilities (e.g., the cross-roll instability) that might close it. These calculations are also beyond the scope of this paper.

A major accomplishment of the present paper has been the demonstration that symmetry-based techniques can be used to solve efficiently modulational instability problems of a substantial degree of complexity. The necessary calculations for the different solutions and lattices show a striking similarity. In particular, the perturbation matrices  $\mathbf{H}_1$ ,  $\mathbf{H}_2$ , and  $\mathbf{H}_3$  are the same for every solution on a lattice and are almost the same among different lattices. The only significant difference among the solutions lies in the lowest order matrix  $\mathbf{H}_0$ . It is therefore hardly surprising that the results for the lamellas are exactly the same on each lattice. Physically, this must be the case. Consider the lamellas on the sc lattice. There is only one kind of phase shift that can take place, namely, shifts in the direction  $\hat{k}_1$ . Because of translation invariance of the lamellas, shifts perpendicular to  $\hat{k}_1$  are identity operations and hence are not associated with a zero eigenvalue. Since the modulation wave vector  $\vec{k}'$  is permitted to point in any direction, the sc calculation already identifies the most general phase modulation; consequently the result using a larger lattice must necessarily be the same. In fact the structure of  $\mathbf{H}_0$  indicates that the  $\alpha_1$  and  $\beta_1$  modes completely decouple from the other modes so that the presence of other lattice wave vectors is irrelevant. There is only one exception: the possibility in two or more dimensions that  $\vec{k}' \perp \hat{k}_1$ , i.e.,  $A=0$  leads to the zigzag boundary at  $q=0$ . However, the directions of the other lattice vectors make no difference and we would get the same answer for any other lattice, including the higher-dimensional representations of the cubic lattices [30].

We also note the similarity of the zigzag boundary  $q=0$  for both the lamellas and the hexagonal prisms. In fact, although the result for the lamellas is the same as that for rolls on two-dimensional lattices, the zigzag boundary for the hexagonal prisms is not found when calculating the stability of hexagons on two-dimensional lattices. This leads to the following.

*Claim.* If the symmetry group  $\Sigma$  of a nontrivial solution  $\mathbf{z}$  contains a continuous translation subgroup, then the solution is unstable to a zigzag instability for  $q<0$ .

Let  $\Gamma$  be the (representation of the) symmetry group of the system of amplitude equations. As explained in Sec. III, in the limit  $k' \rightarrow 0$ , three of the PM eigenvectors of  $\mathbf{H}_0$  correspond to translations in three independent directions. The eigenvalues of  $\mathbf{H}_0$  are exactly the lattice stability eigenvalues, and we know from Ref. [31] that  $\mathbf{H}_0$  must have a null eigenvector for each continuous symmetry of  $\Gamma$  that is *not* in  $\Sigma$ . A continuous translation symmetry that *is* in  $\Sigma$  corresponds to a PM mode that is not generally a null eigenvector of  $\mathbf{H}_0$ . Because  $\mathbf{H}_0$  is Hermitian this PM mode is orthogonal to the null eigenspace of  $\mathbf{H}_0$ . If we choose  $\vec{k}'$  to point in the direction of this continuous translation, then the direction cosines in the orthogonal directions vanish, and the  $(\hat{k}_i \cdot \vec{k}')$  terms in  $\mathbf{H}_1$  and  $\mathbf{H}_2$  *vanish identically* on the null eigenspace of  $\mathbf{H}_0$ . Thus the lowest order perturbation is  $\mathbf{H}_3$ , which always gives instability for  $q<0$ . Because we have chosen  $\vec{k}'$  perpendicular to the direction of the shifts for the null eigenvectors, this is always a zigzag instability.

We therefore conclude that all  $m$ -dimensional patterns in  $n$ -dimensional space ( $m<n$ ) must be unstable to the zigzag instability if the pattern is dilated ( $q<0$ ) from its natural wavelength—its wavelength exactly at onset. In particular, some higher-dimensional representations of the cubic lattice contain higher-dimensional representations of the square lattice, and therefore support prisms based on the patterns found in Ref. [32]. According to the above theorem such prism patterns must also be unstable to the zigzag instability for  $q<0$ .

It is unclear why the same phenomenon should occur for the sc pattern. There is no continuous symmetry, yet there are directions of  $\vec{k}'$  for which  $\mathbf{H}_1$  and  $\mathbf{H}_2$  vanish identically on some portion of the null eigenspace. The terms  $\Delta$ ,  $\Xi$ , and  $Y$  factor into the product of a term independent of  $\lambda$  and  $q$  and a term independent of the direction cosines. This may be due to the high degree of symmetry ( $\langle \phi_i | \mathbf{H}_2 | \phi_j \rangle$  is diagonal, for instance) and the fact that every term in the sc equation for  $z_1$  is proportional to  $z_1$ , a consequence of the absence of spatial resonances among the  $\hat{k}_j$ . This independence of the fundamental wave vectors manifests itself in the structure of the representation of the symmetry group  $\Gamma$ . For example, the  $\Gamma$  for the sc lattice can be written as a *wreath product group* [33,34] but this is not so for the fcc lattice. To write the sc symmetry group as a wreath product we consider the system  $(z_1, z_2, z_3)$  to be the union of three separate subsystems, one for each  $z_j$ , and let  $O(2)$  be the set of rotations (translations) and reflections acting on each amplitude by

$$\tau_\alpha : z_j \rightarrow e^{i\alpha} z_j, \quad \rho : z_j \rightarrow \bar{z}_j.$$

These operations define a local symmetry group, which acts on each individual subsystem. Since these subsystems can be permuted among themselves, an additional (global) symmetry group is present. This is the permutation group  $S_3$ . The wreath product group  $O(2) \wr S_3$  is constructed from these two groups by permitting the local group to act independently on each of the subsystems, much as a local gauge symmetry in field theory. For the sc lattice, the group that results is the group  $\Gamma$ . Evidently this construction requires that the translations for each of the three amplitudes  $z_j$  be independent. This is not so on the fcc lattice, for which the fact that  $\sum_{j=1}^4 \hat{k}_j = \vec{0}$  implies that the actions of the translations on the four amplitudes are not independent, and hence that the symmetry group is not  $O(2) \wr S_4$ .

It appears that it is the presence of such spatial resonances on the fcc and bcc lattices that prevents  $\mathbf{H}_1$  and  $\mathbf{H}_2$  from simultaneously vanishing on the null eigenspace of  $\mathbf{H}_0$ , no matter what the direction of  $\vec{k}'$ . This suggests the following.

*Conjecture.* Let  $G$  be a nontrivial discrete group and let  $\Gamma = O(2) \wr G$ , i.e., the wreath product of  $O(2)$  and  $G$ . Choose a system equivariant under this representation, and let  $\mathbf{z}$  be the solution with all amplitudes equal and nonzero. (A solution of this form is guaranteed by Ref. [34]). Then  $\mathbf{z}$  suffers a zigzag instability for  $q<0$  with  $\vec{k}'$  along a coordinate axis.

Because the isotropy subgroup of this solution [namely,  $\Sigma(\mathbf{z}) = G$ ] is the only axial isotropy subgroup without a continuous symmetry (see Ref. [34]), this conjecture claims that *all* axial solutions on  $O(2) \wr G$  have such a zigzag instability. This conjecture applies to the six-dimensional representation of the sc lattice since  $T^3 \wr O \oplus Z_2 \approx O(2) \wr S_3$ . Here  $O$  is the octahedral group and  $S_3$  the permutation group on three elements. We know of one other instance of this property,

namely, squares on the square lattice, with symmetry  $O(2) \wr Z_2$ . These do indeed undergo exactly this instability [10].

#### ACKNOWLEDGMENT

This work was supported by the National Science Foundation under Grant Nos. DMS-9703684 and DMS-9709494.

- 
- [1] M. C. Cross and P. C. Hohenberg, *Rev. Mod. Phys.* **65**, 851 (1993).
- [2] V. Castets, E. Dulos, J. Boissonade, and P. De Kepper, *Phys. Rev. Lett.* **64**, 2953 (1990).
- [3] P. De Kepper, V. Castets, E. Dulos, and J. Boissonade, *Physica D* **49**, 161 (1991).
- [4] F. S. Bates and G. H. Frederickson, *Phys. Today* **52** (2), 32 (1999).
- [5] K. Staliunas, *Phys. Rev. Lett.* **81**, 81 (1998).
- [6] T. K. Callahan and E. Knobloch, *Phys. Rev. E* **53**, 3559 (1996).
- [7] T. K. Callahan and E. Knobloch, *Nonlinearity* **10**, 1179 (1997).
- [8] M. G. M. Gomes, *Phys. Rev. E* **60**, 3741 (1999).
- [9] L. Kramer and W. Zimmermann, *Physica D* **16**, 221 (1985).
- [10] R. B. Hoyle, *Physica D* **67**, 198 (1993).
- [11] R. B. Hoyle, in *Time-Dependent Nonlinear Convection*, edited by P. A. Tyvand (Comput. Math., Southampton, 1998), pp. 51–82.
- [12] M. M. Sushchik and L. S. Tsimring, *Physica D* **74**, 90 (1994).
- [13] A. C. Newell and J. A. Whitehead, *J. Fluid Mech.* **38**, 279 (1969).
- [14] G. H. Gunaratne, *Phys. Rev. Lett.* **71**, 1367 (1993).
- [15] L. D. Landau and E. M. Lifshitz, *Quantum Mechanics (Non-relativistic Theory)*, 3rd ed. (Pergamon, Oxford, 1977).
- [16] R. Graham, *Phys. Rev. Lett.* **76**, 2185 (1996).
- [17] G. H. Gunaratne, Q. Ouyang, and H. L. Swinney, *Phys. Rev. E* **50**, 2802 (1994).
- [18] T. K. Callahan and E. Knobloch, *Physica D* **132**, 339 (1999).
- [19] T. K. Callahan, Ph.D. thesis, University of California at Berkeley, 1998.
- [20] I. Prigogine and R. Lefever, *J. Chem. Phys.* **48**, 1695 (1968).
- [21] A. De Wit, Ph.D. thesis, Université Libre de Bruxelles, 1993.
- [22] A. De Wit, G. Dewel, P. Borckmans, and D. Walgraef, *Physica D* **61**, 289 (1992).
- [23] I. Lengyel and I. R. Epstein, *Science* **251**, 650 (1991).
- [24] I. Lengyel and I. R. Epstein, in *Chemical Waves and Patterns*, edited by R. Kapral and K. Showalter (Kluwer, Dordrecht, 1995), pp. 297–322.
- [25] S. Fauve, in *Instabilities and Nonequilibrium Structures*, edited by E. Tirapegui and D. Villarroel (Reidel, Dordrecht, 1985), pp. 63–88.
- [26] B. Echebarría and C. Pérez-García, *Europhys. Lett.* **43**, 35 (1998).
- [27] M. Golubitsky, J. W. Swift, and E. Knobloch, *Physica D* **10**, 249 (1984).
- [28] R. M. Clever and F. H. Busse, *Phys. Rev. E* **53**, R2037 (1996).
- [29] H. Riecke, *Europhys. Lett.* **11**, 213 (1990).
- [30] B. Dionne and M. Golubitsky, *ZAMP* **43**, 36 (1992).
- [31] M. Golubitsky, I. Stewart, and D. G. Schaeffer, *Singularities and Groups in Bifurcation Theory* (Springer-Verlag, Berlin, 1988), Vol. II.
- [32] B. Dionne, M. Silber, and A. C. Skeldon, *Nonlinearity* **10**, 321 (1997).
- [33] A. P. S. Dias, *Nonlinearity* **11**, 247 (1998).
- [34] B. Dionne, M. Golubitsky, and I. Stewart, *Nonlinearity* **9**, 559 (1996).